

**REGIONAL MAGNETIC DATA ANALYSIS FOR  
METALLIC ORE DETECTION WITHIN  
STRUCTURAL ASSEMBLAGES OF MUSLIM BAGH  
OPHIOLITE BELT BALOCHISTAN**



**By  
NASRULLAH (021102113020)  
M.Phil. Geophysics (2021 - 2023)**

**Department of Earth Sciences  
Quaid-i-Azam University Islamabad, Pakistan**

بِسْمِ اللَّهِ الرَّحْمَنِ الرَّحِيمِ

*To start with the greatest name of Almighty Allah. Most gracious and merciful, with Him is the knowledge of the Hour, He sends down the rain, and knows that which is in the wombs. No person knows what he will earn tomorrow, and no person knows in what land he will die. The knower of the unseen is Allah these are the keys of the unseen, whose knowledge Allah alone has kept for himself and no one else knows them unless Allah tells him about them.*

## **CERTIFICATE**

It is certified that Nasrullah Khan s/o Haji Ghulam Rasool carried out the work contained in this dissertation under my supervision and accepted in its present form by Department of Earth Sciences, Quaid-i-Azam University Islamabad, Pakistan as satisfying the requirements for M.Phil. degree in Geophysics.

### **RECOMMENDED BY:**

**Prof. Dr. Aamir Ali** \_\_\_\_\_

Supervisor

Department of Earth Sciences

QAU, Islamabad.

**Prof. Dr. Mumtaz Muhammad Shah** \_\_\_\_\_

Chairman

Department of Earth Sciences

QAU, Islamabad.

**External Examiner** \_\_\_\_\_

## **DEDICATION**

To my Parents, siblings and my spouse and children (My lovely daughters: Ayesha, Summaya, Omeera, and Nabila) without your prayers and support and your trust in me it was not possible for me to achieve this kind of success. May Allah always keep your prayers with me and shower His blessings upon you guys.

Secondly, I want to dedicate this thesis to Department of Earth Sciences QAU Islamabad, you have taught me a lot.

## **ACKNOWLEDGMENT**

In the name of Allah, the most Beneficent, the most Merciful. All praises to Almighty Allah, the creator of universe. Secondly, my humblest gratitude to the Holy Prophet Muhammad (Peace Be Upon Him). Without the blessing of Allah, I could not be able to complete my work as well as to be at such a place. This thesis appears in its current form due to the assistance and guidance of several people. It gives me great pleasure to express my gratitude to all those who supported me and have contributed to making this thesis possible.

I express my profound sense of reverence to Dr. Aamir Ali, The Professor, who gave me the opportunity to work under his supervision on such outstanding research. His continuous support, motivation and untiring guidance have made this thesis possible. His vast knowledge, calm nature and positive criticism motivated me to push harder to get the best forms of results. I thank him for bearing my mistakes and being the “teacher” that many fails to understand the true concept of this elevated post bestowed upon them.

Also, I am immensely pleased to place on record my deep gratitude and heartfelt thanks to Sami-Ur-Rehman, Muhammad Kamran Chughtai, Yawar Amin, Farman Ullah, Irfan Haider, Hassan Zahid and Mishal Razzaq who helped me during this research , and my friends and many others without whom this course work would have been hard to be completed.

Last but not least, I would like to acknowledge my family for their constant support, unceasing prayers and best wishes. My parents, brothers (Abdullah Wadan, Amanullah, Faizullah, Najeebullah & Naseebullah) and sisters. I thank the most who helped me most with their constant support throughout the time for the successful completion of my thesis. Those missed to be named are always close to my heart, and if not named in the acknowledgment are fully thanked.

**NASRULLAH**

**MPHIL GEOPHYSICS**

**2021-2023**

## ABSTRACT

The application of regional magnetic survey is a key geophysical technique utilized to detect subsurface magnetized zones that hold potential for exploratory purposes. In the domain of geophysics, the detection of anomalous magnetization has the potential to suggest the presence of localized mineral deposits, which could hold economic importance. Hence, an assessment and analysis were conducted on a dataset comprising magnetic measurements obtained from the Muslim Bagh ophiolite region located in Balochistan. The Muslim Bagh ophiolite belt comprises many ophiolite zones that delineate the boundary separating the Afghan block of the Eurasian plate from the Indian plate. During the Late Cretaceous period, the ophiolites accreted onto the Indian continental margin.

The purpose of the investigation was to ascertain and pinpoint areas of anomaly within the specified study area. The study site is situated in a latitude of 30 degrees, 49 minutes, and 27 seconds North, and a longitude of 67 degrees, 44 minutes, and 2 seconds East, within the ophiolitic belt of Muslim Bagh. A total of 1012 magnetic measurements from toposheets 34N/9 and 34N/13 were utilized for the purpose of study. The data were collected using a Proton Precession Magnetometer G-856AX. The collected data are presented in the form of 2D contour magnetic anomaly maps and total magnetic intensity (TMI) maps. Additionally, a 3D anomaly map was created to aid in the qualitative interpretation of the data. The field data were analyzed using Surfer and Geosoft software, which allowed for the creation of two cumulative maps: one for magnetic anomaly and one for total magnetic intensity (TMI). These maps revealed the presence of two distinct magnetic anomalous zones within the study area.

The area under consideration exhibits a significant level of anomaly, as evidenced by the magnetic anomaly values recorded, which range from 520 to 2480 nanotesla. The other low anomalous zone exhibited magnetic field values ranging from -40 to -600 nanotesla. A cumulative total magnetic intensity (TMI) map was created, which identified and emphasized two magnetic zones (one high and one low) in order to validate the anomalous zones indicated on the cumulative magnetic anomaly map. The TMI values of the high magnetic zone exhibited a range between 48620 nT and 50540 nT. The observed higher magnetic readings are indicative of the presence of metallic mineralization. The TMI

values of the low magnetic zone exhibited fluctuations ranging from 47500 nT to 47980 nT, indicating the absence of magnetic properties in the subsurface. The high magnetic anomaly zone is observed to extend from toposheet 34N/9 to 34N/13 in a southwest to northeast direction.

Additionally, the overall intensity map was divided into maps depicting regional anomalies and residual anomalies. The residual anomaly map underwent processing, incorporating several properties including Reduction to Equator, Vertical and Horizontal derivatives, and upward continuation. These techniques were employed to accurately identify anomalous zones and enhance the understanding of magnetic data. Therefore, the utilization of integrated geophysical techniques and thorough investigations can yield vital information regarding the identification of promising zones and the spatial distribution of magnetic minerals within the designated study region.

# Table of Contents

CERTIFICATE.....	ii
DEDICATION .....	iii
ACKNOWLEDGMENT.....	iv
ABSTRACT.....	v
LIST OF FIGURES .....	xii
CHAPTER 01 .....	1
INTRODUCTION .....	1
1.1 Introduction .....	2
1.2 Study Area .....	4
1.3 Climate and weather conditions .....	6
1.4 Objectives.....	6
1.5 Data Source .....	6
1.5.1 Data Set.....	6
1.5.2 Base Map of Toposheets No. 34N/9 & 34N/13 .....	7
1.6 Methodology .....	8
CHAPTER 02 .....	9
GEOLOGY AND STRATIGRAPHY .....	9
2.1 Introduction .....	10
2.2 Stratigraphy of study area .....	11



2.2.1	Nisai Formation .....	13
2.2.2	Khojak Formation .....	13
2.2.3	Murgha Faqirzai Member .....	13
2.2.4	Shaigalu Member .....	14
2.2.5	Dasht Murgha Group .....	15
2.2.6	Malthanai Formation.....	15
2.2.7	Bostan Formation.....	16
2.2.8	Zhob valley deposits .....	16
2.3	Muslim Bagh Ophiolite.....	16
2.4	The ultramafic rocks north of Muslim Bagh (Shina Khwara) .....	17
CHAPTER 03 .....		19
MAGNETIC DATA ACQUISITION AND PROCESSING .....		19
3.1	Introduction .....	20
3.2	Survey Planning .....	21
3.3	Data Acquisition in Semi-Detailed Survey .....	21
3.4	INSTRUMENTS USED .....	22
3.4.1	Magnetometer .....	22
3.4.2	Hand-held GPS .....	23
3.5	Acquisition Parameters .....	24
3.5.1	Recording Parameters .....	24

3.6	Precautions .....	24
3.7	Magnetic Data processing .....	25
3.7.1	Introduction.....	25
3.7.2	Diurnal variation .....	25
3.7.3	Normal Correction .....	26
3.7.4	Reduction to Equator .....	26
3.7.5	Upward Continuation.....	27
3.7.6	First Order Vertical Derivative.....	28
3.7.7	Horizontal Derivative.....	28
CHAPTER 04 .....		29
INTERPRETATION AND ANALYSIS OF MAGNETIC DATA .....		29
4.1	Introduction .....	30
4.2	Qualitative Interpretation .....	31
4.3	Gridding .....	31
4.4	Division of Data .....	31
4.5	Semi-Detailed Magnetic Data Interpretation of Toposheet 34N/9.....	31
4.5.1	Magnetic Anomaly Map of Toposheet No. 34N/9.....	32
4.5.2	Total Magnetic Intensity (TMI) Map of Toposheet No. 34N/9 .....	33
4.6	Semi-Detailed Magnetic Data Interpretation of Toposheet 34N/13.....	34
4.6.1	Magnetic Anomaly Map of Toposheet No. 34N/13 .....	34

4.6.2	Total Magnetic Intensity (TMI) Map of Toposheet No. 34N/13 .....	35
4.7	Semi-Detailed Magnetic Data Interpretation of Combined Toposheets (34N/9 & 34N/13) .....	36
4.8	Cumulative Total Magnetic Intensity (TMI) Map.....	37
4.9	3D Visualization of Cumulative Anomaly Map .....	38
4.10	TMI Map of Digitized High Anomalous Zone .....	39
4.11	Superposition of Digitized Anomalous Zone and Geological Map of Study Area 40	
CHAPTER 05 .....		42
MAGNETIC ATTRIBUTES.....		42
5.1	Introduction.....	43
5.2	Residual Magnetic Anomaly Map .....	44
5.3	Interpolated Residual Magnetic Anomaly Map .....	45
5.4	Reduced to Magnetic Equator (RTE) Anomaly Map.....	46
5.5	Upward Continuation Map .....	48
5.6	First Order Vertical Derivative Map .....	49
5.7	Horizontal Derivative Map .....	50
CHAPTER 06 .....		52
DISCUSSIONS, CONCLUSIONS AND RECOMMENDATIONS .....		52
6.1	Discussions .....	53

6.2	Conclusions.....	55
6.3	Recommendations.....	55
	REFERENCES .....	56

## LIST OF FIGURES

Figure 1.1: Study Area Map: (a) Represents Pakistan on the globe. (b) Highlights Zhob Division in which study area is lying. (c) Shows Muslim Bagh (Study Area).....	4
Figure 1.2: Location map (Google map) of the study area, highlighting Jang Tor Ghar Massif, Saplai Tor Ghar Massif, and Ultramafic rocks. ....	5
Figure 1.3: (a) and (b) Indicate base maps of toposheets 34N/9 & 34N/13 respectively, red circular dots represent magnetic measurements in the study area. ....	7
Figure 1.4: Flow chart of methodology used in this research.....	8
Figure 2.1: The study area geological map (Modified from Geological Canadian Map No. 26 Quetta 34 J-N. ....	11
Figure 2.2: Proposed lithostratigraphy and tectono-stratigraphic zones of the study and surrounding area (Kasi et al., 2012).....	12
Figure 3.1: Magnetic data acquisition base map of study area showing survey points along various profiles in the study area.....	21
Figure 3.2: G-856AX Geometrics Proton Precision Magnetometer used for magnetic data acquisition. ....	23
Figure 3.3: Garmin hand-held GPS used to determine the coordinates of the observation stations. ....	23
Figure 4.1: Magnetic anomaly map of toposheet 34N/9 showing high and low magnetic anomalous zones with rectangles (a) & (b) respectively. ....	32
Figure 4.2: Total Magnetic Intensity (TMI) map of toposheet 34N/9 showing high and low magnetic zones with rectangles (a) & (b) respectively. ....	33
Figure 4.3: Magnetic anomaly map of toposheet 34N/13 depicting high and low anomalous zones marked with rectangles (a) & (b) respectively.....	34
Figure 4.4: Total Magnetic Intensity (TMI) map of toposheet 34N/13 depicting high and low magnetic zones marked with rectangles (a) & (b) respectively. ....	35

Figure 4.5: Cumulative magnetic anomaly presentation of toposheets (34N/9 & 34N/13) highlighting high and low anomalous zones with arrows. .... 36

Figure 4.6: Cumulative total magnetic intensity (TMI) display of toposheets (34N/9 & 34N/13) indicating high and low magnetic zones with rectangles as described in the figure. .... 37

Figure 4.7: 3D Visualization of cumulative magnetic anomaly which clearly separates magnetic highs and lows as marked in the figure. .... 38

Figure 4.8: Digitized TMI map specifying high magnetic/ anomalous zone indicated by rectangles (a), (b), (c) and in the study area. .... 39

Figure 4.9: Overlay of high magnetic zone on geological map of study area highlighting zone of interest. .... 40

Figure 5.1: Residual magnetic anomaly map highlighting magnetic observation points. Pink color indicates higher residual magnetic anomalies while blue color lower anomalies. .... 45

Figure 5.2: Interpolated Residual Anomaly map with location plots. Black dots represent high magnetic readings and white triangles low magnetic values. .... 46

Figure 5.3: Shows residual magnetic anomaly reduced to equator. The map clearly delineates high and low magnetized zones marked with black and white dotted polygons respectively. .... 47

Figure 5.4: Reduced to Equator anomaly upward continued to 300 m elevation. It separated anomalous zones into distinct high magnetized zones. .... 48

Figure 5.5: First order vertical derivative map representing distinct high and low anomalous zones with black and white polygons respectively. The distinct high anomalous zones are highlighted with arrows. .... 49

Figure 5.6: Horizontal derivative map representing variation of magnetic intensity values spatially within the study area. Black dotted polygons indicate high magnetized zone and white polygons the lower magnetized zone. .... 50

## **CHAPTER 01**

### **INTRODUCTION**

## 1.1 Introduction

The magnetic method, which is regarded as one of the oldest geophysical exploration techniques, had substantial expansion subsequent to the use of airborne surveys during World War II. The thorough mapping of the entire crustal section across different scales has been made possible by advancements in equipment, navigation, and platform adjustment (Nabighian et al., 2005). This encompasses the capability to delineate highly magnetic subsurface formations on a larger geographical scale, as well as identifying less magnetic sedimentary boundaries on a smaller, more localized level. Significant breakthroughs have been made in the approaches for data filtering, display, and interpretation, mostly attributed to the increased availability of affordable, color raster graphics and high-performance personal computers (Nabighian et al., 2005).

Magnetic methods play a significant role in various fields of study, including ore and mineral exploration (Essa and Elhussein; Amoah et al., 2018; 2019; Abedi et al., 2013), hydrocarbon exploration (Al-Farhan et al., 2019; Abubakar et al., 2015), archaeology investigation (Di Maio et al., 2018), hydrogeology (Essa et al., 2015; Araffa et al., 2017; Al-Garni, 2011), geothermal exploration (Abdel Zaher et al., 2018; Aboud et al., 2011), engineering applications (Bin et al., 2009), unexploded ordnance (UXO) delineation (Wu et al., 2015), buried paleo-channels (Maus et al., 1999), paleo-shear zones (Dunstan et al., 2016), and structural lineaments analysis (Elhussein and Shokry, 2020; Middleton et al., 2015).

Magnetic exploration, also known as "potential field" exploration, is employed as a means for geoscientists to gain an indirect understanding of subsurface structures by detecting the magnetic properties of rocks. The utilization of the magnetic technique in exploration endeavors can facilitate the identification and localization of mineral deposits. The utilization of potential field survey techniques offers a cost-effective means of efficiently surveying extensive land expanses. The approach is cost-effective, minimally intrusive, and environmentally benign (Adagunodo et al., 2015).

The Balochistan Basin is widely recognized as one of the most affluent basins in terms of its abundant mineral reserves (Malkani et al., 2017). The Chagai-Raskoh-Wazhdad magmatic arc, situated within the Balochistan basin, together with the Western Indus



Suture, which lies on the eastern border of the Balochistan Basin, are recognized as highly prolific metallogenic zones. The Balochistan Basin possesses substantial confirmed reserves of domestic iron, copper (along with certain amounts of gold, silver, molybdenum), lead, zinc, barite, chromite, limestone/marble, and other minerals. Additionally, it contains minor concentrations of antimony, asbestos, magnesite, soapstone, sulphur, vermiculite, and other minerals. According to Malkani et al. (2017), certain commodities are currently being utilized and exported, whereas the majority of commodities are currently awaiting utilization and further development.

Muslim Bagh, located in the province of Balochistan, is widely renowned for its significant chromite mining activities. The region exhibits many mineral showings and deposits, including chromite, copper, iron ore, graphite, fluorite, manganese, magnesite, nickel, asbestos, platinum, serpentine, and talc (Kazmi & Abbas, 2001).

A semi-detailed magnetic survey was done in the Muslim Bagh ophiolitic belt and its surrounding regions with the aim of identifying metallic minerals and delineating places with significant mineral deposits. Data of two complete topographic sheets, namely 34N/9 and 34N/13, were processed and utilized for the purpose of visualizing and interpreting magnetic anomalous zones. 2D contour maps were constructed using regional magnetic anomaly and total magnetic intensity (TMI) measurements. The toposheet 34N/9 encompasses a region characterized by a prominent magnetic anomaly, exhibiting a maximum anomaly value of approximately 2550 nT. Additionally, the total magnetic intensity (TMI) value inside this area is estimated to be around 50500 nT. The toposheet 34N/13 encompasses a region characterized by a relatively weak magnetic field, as seen by a narrow range of magnetic anomaly values centered around -600 nanotesla, and a total magnetic intensity (TMI) value of 47300 nanotesla.

Several magnetic attributes, including horizontal and vertical derivatives, Upward Continuation, and Reduction to Equator (RTE), were utilized to produce residual magnetic anomaly maps. These maps were generated with the aim of improving the visualization of the zones of interest and facilitating a more meaningful interpretation of the data.

## 1.2 Study Area

The study location under consideration is Muslim Bagh, renowned for having Pakistan's most prominent ophiolite deposits. The geographical location of the area under consideration is situated inside the Zhob division and Killa Saifullah district of Balochistan province, as depicted in Figure 1.1. The study site is located approximately 110 kilometers away from Quetta, positioned in the east-northeast direction of the city.

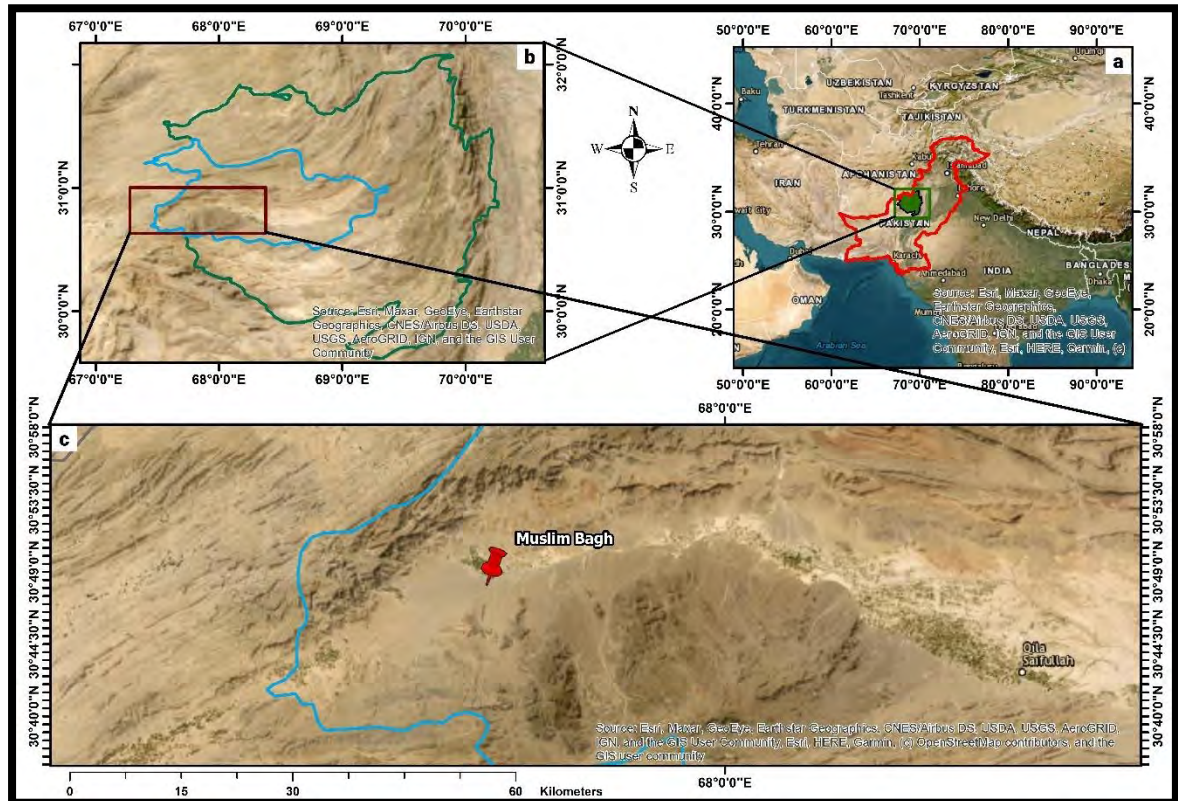


**Figure 1.1:** Study Area Map: (a) Represents Pakistan on the globe. (b) Highlights Zhob Division in which study area is lying. (c) Shows Muslim Bagh (Study Area)

The Muslim Bagh Ophiolites form an integral component of the Zhob Valley Ophiolites, situated in the eastern-northeastern region of Balochistan, in close proximity to Quetta. The Muslim Bagh Ophiolites have significant presence in the southeastern region of Muslim Bagh, specifically within the Jang Tor Ghar Massif and the Saplai Tor Ghar-Nisai Massif (Figure 1.2). The Saplai Tor Ghar-Nisai Massif spans an area of approximately 600 square kilometers and reaches a maximum elevation of 2700 meters. In contrast, the

Jang Tor Ghar Massif encompasses an estimated 150 square kilometers and has a peak elevation of 3010 meters (Farah and DeJong, 1979).

The research area encompasses ultramafic rock formations located to the north of Muslim Bagh inside the Shina Khwara region. The ultramafic rocks found in Shina Khwara exhibit a high degree of tectonization, which sets them apart from the ultramafic rocks found in the Jang Tor Ghar Massif and Saplai Tor Ghar Massif in the southern region (Figure 1.2). The geographical positioning suggests that the allochthonous masses of the south Muslim Bagh complex have their origins in the northern region (Farah and DeJong, 1979).

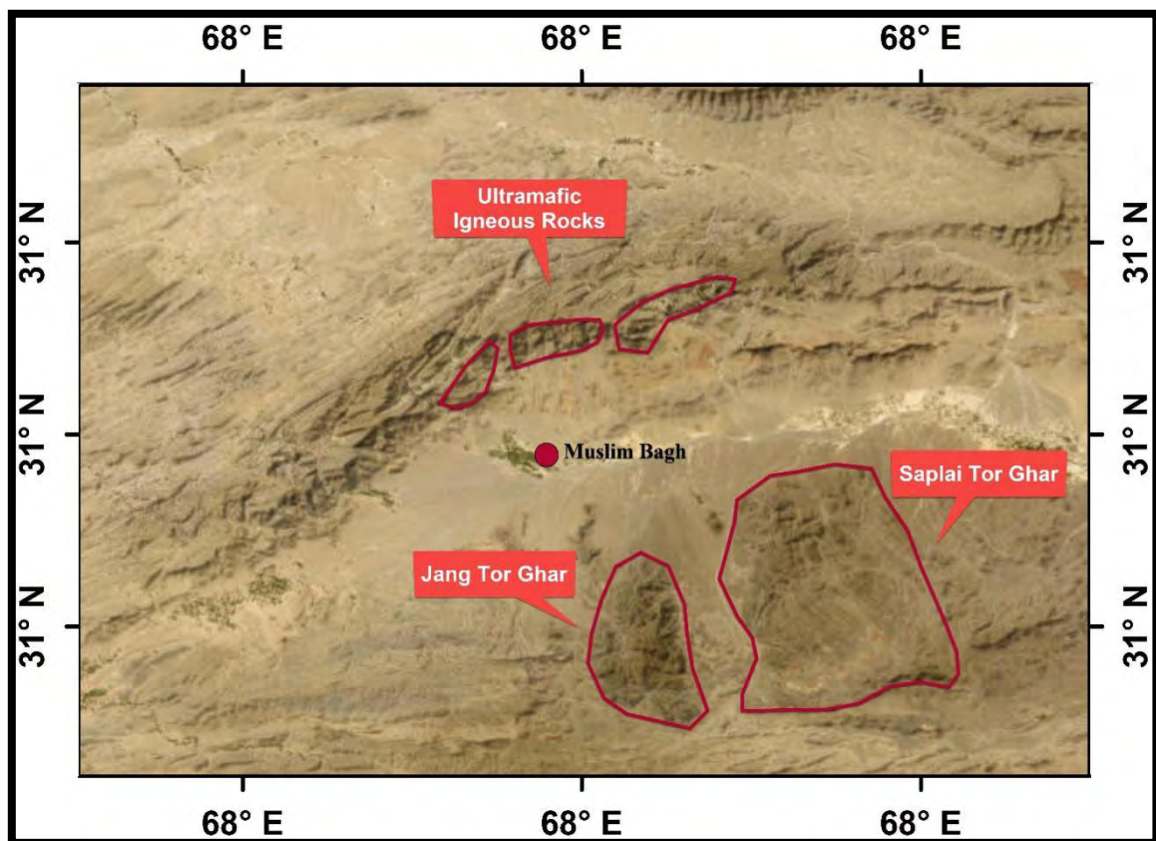


**Figure 1.2:** Location map (Google map) of the study area, highlighting Jang Tor Ghar Massif, Saplai Tor Ghar Massif, and Ultramafic rocks.

Muslim Bagh, formerly known as Hindu Bagh prior to 1971, is a small mining town situated in a geographical position of latitude 30°49'27"N and longitude 67°44'2"E. It is situated at an elevation of 1860 meters (Farah and DeJong, 1979).

### **1.3 Climate and weather conditions**

The winters in Muslim Bagh and its surrounding regions are characterized by cold temperatures and a duration that spans seven months. In contrast, the summers are characterized by moderate temperatures and a duration that spans five months. The temperature range often seen falls between the interval of 15 to 20<sup>0</sup> degrees Celsius. The greatest recorded maximum temperature reaches 43<sup>0</sup> degrees Celsius during the month of June, while the lowest recorded maximum temperature falls below -90 degrees Celsius in the month of January.

### **1.4 Objectives**

- To analyze and interpret the semi detailed magnetic data in order to demarcate high and low magnetic zones which are favorable indications of magnetic and non-magnetic mineralization in the acquired area.
- To identify potential minerals and resources by detecting magnetic signatures associated with ore deposits.
- Creation of magnetic anomaly maps to visualize and understand the distribution and characteristics of magnetic features.
- To obtain comprehensive understanding of the magnetic properties of a study area.

### **1.5 Data Source**

To carry out research work in Muslim Bagh area, data were provided by Geological Survey of Pakistan. Details of data used for the study area are as under:

- Longitude and Latitude values of measured readings
- Time values (in hours and minutes)
- Base station observed readings
- Measured magnetic field readings

#### **1.5.1 Data Set**

The Geological Survey of Pakistan has released the data of two complete toposheets for the purpose of research. A toposheet, alternatively referred to as a topographic map, is

a detailed cartographic representation that provides accurate details pertaining to the topography, characteristics of the terrain, and geographic features of a specified area. A comprehensive set of 1012 magnetic readings were obtained and subsequently utilized to generate individual base maps for each toposheet.

### 1.5.2 Base Map of Toposheets No. 34N/9 & 34N/13

In the discipline of geophysics, a base map is considered an essential cartographic depiction that typically presents essential geographical and topographical information related to a certain area. The entity indicated above serves as a reference point for various geophysical studies and assessments. The maps stated above provide significant contextual and spatial information that aids in the analysis and interpretation of geophysical data collected during field research. Figure 1.3 depicts the magnetic values acquired from two specific topographic sheets within the chosen area of investigation. Toposheet (a) comprises a total of 563 data points, whilst toposheet (b) encompasses 449 data points. The data collection for this study is undertaken on various routes that are easily accessible, encompassing both paved and dirt roads, with differing profile directions.

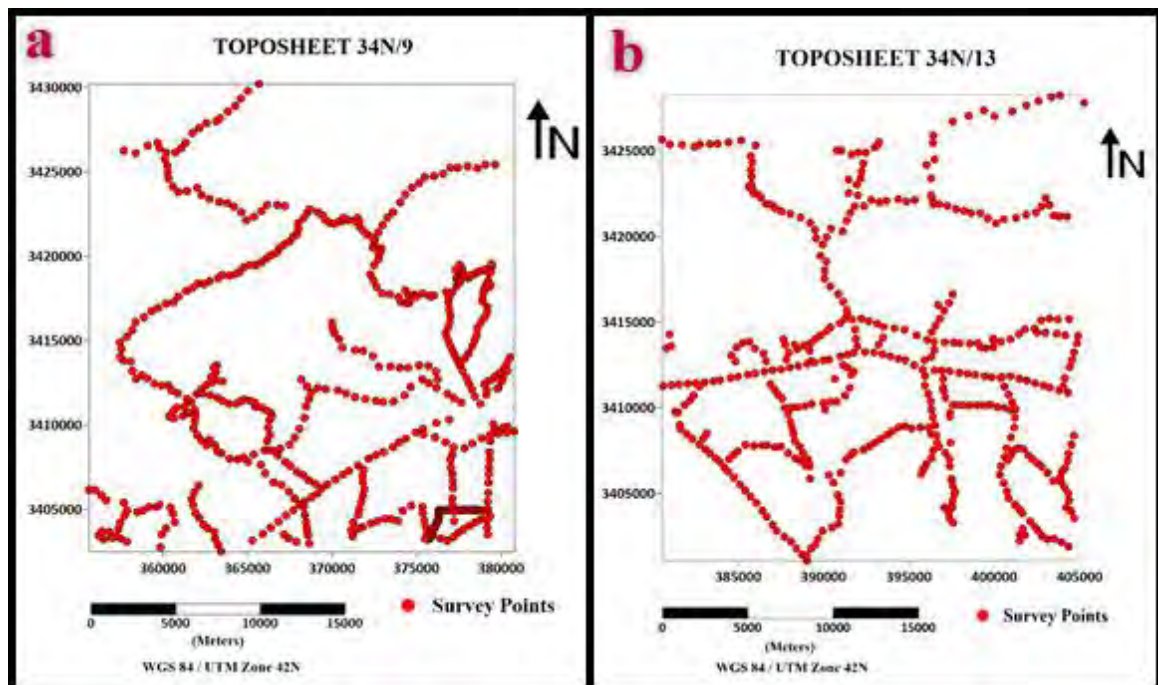


**Figure 1.3:** (a) and (b) Indicate base maps of toposheets 34N/9 & 34N/13 respectively, red circular dots represent magnetic measurements in the study area.

## 1.6 Methodology

This study employs a thorough methodology with the objective of enhancing the understanding of magnetic data. The methodology began with a comprehensive analysis of magnetic data in order to identify and rectify any potential inaccuracies. The second phase of the experiment encompassed the data processing stage, which entailed the elimination of diurnal fluctuations in the recorded data and the adjustment for the influences of latitudinal and longitudinal factors. In the third stage, the data underwent preparation in order to generate 2D maps depicting the total magnetic intensity and anomaly contours. These maps were utilized to delineate regions characterized by high and low magnetic values, facilitating a qualitative interpretation of the data. The fourth stage involved the partitioning of the overall magnetic intensity into regional and residual anomalies. The fifth stage involved the utilization of many techniques, including reduction to the equator, calculation of horizontal and vertical derivatives, and the process of upward continuation over the residual anomaly map. These methods were employed to improve and refine the interpretation of the data. Flow chart of methodology is given in (Figure 1.4).

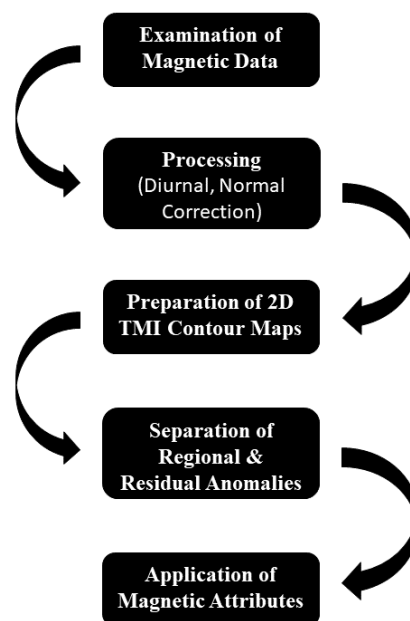


**Figure 1.4:** Flow chart of methodology used in this research.

**CHAPTER 02**  
**GEOLOGY AND STRATIGRAPHY**

## 2.1 Introduction

From a tectonic perspective, the geological composition of the Muslim Bagh region (as depicted in Figure 2.1) can be classified into three discrete geological terranes. The Pishin Flysch Belt, Khanozai-Muslim Bagh Ophiolite Complex situated in the suture zone, and the Calcareous Belt are the geological formations observed in a north to south orientation. The initial classification of the area was conducted by Iqbal (2004), who identified three distinct zones: The Calcareous zone, the Axial zone, and the Flysch zone. The Pishin Flysch belt is located to the north of the ophiolite suture belt. The flysch zone is thereafter categorized into six discrete tectonostratigraphic zones. The oldest and lowest geological formation is referred to as the Late Cretaceous Muslim Bagh Ophiolite zone I, as identified by Kasi et al. in 2012. The individuals that inhabit this particular area are readily apparent inside the vicinity of Zhob valley. The Muslim Bagh ophiolite, which is extensively exposed, is situated in the southeastern extension of the ophiolitic belt. This belt encompasses Bela, Muslim Bagh, Zhob, and Waziristan, and is positioned at the northwestern edge of the Indian Continental margin (Siddiqui et al., 1996; Jadoon & Khurshid, 1996;). The initial description and mapping of the subject were conducted by Vredenburg in 1901. Jones (1961) subsequently produced a reconnaissance map of the Muslim Bagh ophiolites. Rossman et al. (1971) produced a comprehensive cartographic representation of the encompassing region. In a subsequent study, Khan et al. (2007) employed Geographic Information Systems (GIS) and remote sensing techniques to provide a comprehensive cartographic representation of the Muslim Bagh ophiolites, marking the first instance of such an approach being utilized. The Ophiolites Muslim Bagh are believed to represent segments of the Neo Tethys, which were thrust upon the advancing Indian Plate during the demise of Neo-Tethys ocean and the consequential event at the Cretaceous-Tertiary boundary of the renowned Eurasian plate (Gnos et al., 1997; Ahmed, 1996; Sarwar, 1992; Allemann, 1979). The emplacement of the Muslim Bagh Ophiolite occurred approximately 65-70 million years ago, as determined by age dating using the  $^{40}\text{Ar}/^{39}\text{Ar}$  method (Mahmood et al., 1995). The Muslim Bagh Ophiolite is comprised of a comprehensive assemblage of ophiolitic rocks, encompassing gabbro pillow basalts, cumulates, ultramafic tectonites, and pelagic sediments that overlie them (Khan et al., 2007).



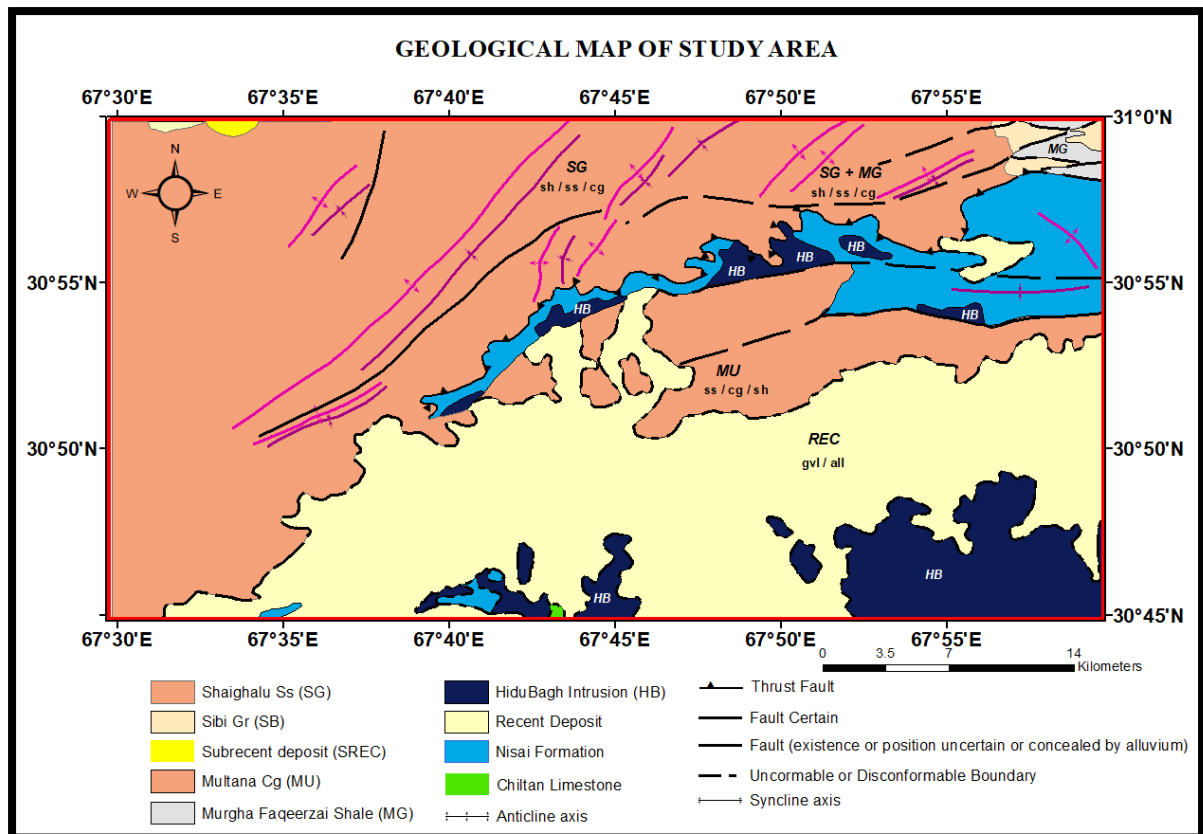


Figure 2.1: The study area geological map (Modified from Geological Canadian Map No. 26 Quetta 34 J-N).

## 2.2 Stratigraphy of study area

The stratigraphic succession of the study area encompasses several geological formations, arranged in chronological order from oldest to youngest. These formations include the Eocene Nisai formation, followed by the Oligocene to early Miocene Khojak formation, which comprises the Murgha Faqeerzai and Shaighalu members. The middle-late Miocene Dasht Murgha group is next in the sequence, followed by the late Miocene to Pliocene Maltani formation. Lastly, the Pleistocene Bostan formation concludes the stratigraphic succession (Figure 2.2). The geological feature under consideration is a regionally extensive southeast convex band characterized by a broad structural configuration and the presence of several thrust-bound zones. The belt discussed has undergone folding processes, resulting in the creation of wide synclines and narrow anticlines (Iqbal, 2004). These structural features are indicative of transgressive to compressional deformation patterns. The belt in question has undergone translation towards

the southeast, specifically along the Zob thrust located at the western passive limit of the Indian plate (Troloar and Izzat, 1993; Lawrence and Yeats, 1979; Raza and Bender, 1995; Lawrence et al., 1981; Kazmi and Jan, 1997). The research field exhibits clear lithostratigraphy and may be categorized into 06 tectono-stratigraphic zones, which are demarcated by significant thrusts and unconformities (HSC, 1960; Kasi et al., 2012). The following are many illustrative instances: The Muslim Bagh-Zhob ophiolites, which are situated in close proximity to the northwestern periphery of the Indian tectonic plate, delineate a significant geological feature. Zone I. Zone-II comprises the Eocene Nisai formation (Cheema et al., 1977; Hunting survey corporation, 1960) and the Oligocene early Miocene Khojak formation (Raza and Bender, 1995), which is situated above Zone-I. Zone-III encompasses the Miocene Dasht Murgha Group, Zone-IV comprises the late Miocene-Pliocene Malthanai formation, Zone-V encompasses the Pleistocene Bostan formation, and Zone-VI comprises the Zhob valley deposits, which are distributed extensively across the Zhob valley region. The subsequent passages provide detailed accounts of the primary lithostratigraphic units within the research area.

Age	Group	Formation/Member	Lithology	Tectono-stratigraphic Zones
Holocene	-	Zhob River Deposits	Conglomerate, sandstone and shale / siltstone	Zone VI
		<b>Thrust</b>		
Pleistocene	-	Bostan Formation	Red colored shale/siltstone, conglomerate and sandstone	Zone V
		<b>Thrust</b>		
Late Miocene-Pliocene	-	*Malthanai Formation	Sandstone/conglomerate interbedded with red colored mudstone/siltstone	Zone IV
		<b>Thrust</b>		
Middle to Late Miocene	**Dasht Murgha Group	Sra Khula Formation Bahlol Nika Formation Khuzhobai Formation	Dark red Mudstone dominated cyclic alteration of mudstone, siltstone and sandstone Dominantly greyish green sandstone, with subordinate mudstone and occasional conglomerate Dominantly maroon mudstone with subordinate reddish brown sandstone	Zone III
		<b>Thrust</b>		
Oligocene – Early Miocene	-	Shaigalu Member Khojak Formation Murgha Faqirzai Member	Dominantly sandstone with subordinate shale Dominantly shale with subordinate sandstone	
Eocene	-	Nisai Formation	Highly fossiliferous to reefoid limestone interbedded with marl and shale and thick marine (fossiliferous) shale with occasional thin limestone horizons	Zone II
		<b>Nonconformity</b>		
Cretaceous	-	Muslim Bagh-Zhob Ophiolite	Mostly ultrabasic and basic igneous rocks	Zone I

**Figure 2.2:** Proposed lithostratigraphy and tectono-stratigraphic zones of the study and surrounding area (Kasi et al., 2012)

### **2.2.1 Nisai Formation**

The Nisai Formation is observed to be in a non-conformable relationship with the Muslim Bagh Ophiolites. The Nisai formation was designated by the Hunting Survey Corporation (1960) in reference to the Nisai town, which corresponds to the preceding nummulitic strata described by Davies (1930) and the black nummulitic limestone identified by Vredenburg (1904). The Nisai formation was designated by Chemma et al. (1977). The formation, located approximately 12 kilometers north of Nisai railway station, exhibits a thickness of 1200 meters, as reported by HSC (1960). The Nisai formation exhibits its most visibility in the Zhob valley thrust, specifically in the Sharan Jogazai region located to the west of the Dasht Murgha syncline. The geological composition of the formation consists primarily of limestone, shale, with subordinate occurrences of sandstone, conglomerate, and marl. The limestone exhibits characteristics of being argillaceous and has a brownish grey coloration. Sandstone exhibits a greenish grey hue and possesses diminutive granules, while shale is characterized by its calcareous composition, fissile nature, and pale grey to greenish coloration. The Nisai Formation, in conjunction with the Khojak Formation, is categorized as zone II.

### **2.2.2 Khojak Formation**

The nomenclature of the Khojak formation was derived from its association with the Khojak pass in close proximity to Chaman. This designation was initially proposed by Vredenburg in 1909, who classified it as the Khojak shale. The Murgha Faqirzi component represents a succession characterized by lower shale dominance, whereas the Shaigalu member is characterized by an upper Shaigalu sandstone dominance. The thickness of the Khojak formation is approximately 6300 meters.

### **2.2.3 Murgha Faqirzai Member**

The shale component known as Murgha Faqirzai is so named due to its association with the settlement of Murgha Faqirzai located in the Killa Saifullah area. The section known as Rud Faqirzai, with a thickness of 2000 m, is widely recognized as the primary reference section for the Murgha Faqirzai member, as documented by Jones in 1961. The composition primarily consists of shale (or slate) with a greenish grey to olive grey hue,

interspersed with siltstone, sandstone, and sporadic layers of shaly limestone. According to the Hunting Survey Corporation (1960), an Oligocene age was given to foraminifera. The current member is situated in a transitional and conformable manner on the Nisai formation, and its upper boundary with the Shaigalu member exhibits a similar transitional nature.

#### **2.2.4 Shaigalu Member**

The appellation "Shaigalu" was bestowed upon the military facility situated around 50 kilometers southwest of Zhob town, thereby establishing a nomenclatural association. The reference section of the Shaigalu member also includes information from the Hunting Survey Corporation in 1960. The Shaigalu component consists predominantly of sandstone, with a minor presence of interbedded shale. The sandstone exhibits a light grey to greenish grey coloration, displaying a medium to coarse grain size. It is characterized by variable bed thickness, ranging from thick to thin, with certain layers measuring up to 10 meters in thickness. Shale exhibits a pale green coloration, possesses a calcareous composition, and displays a flaky texture. In the Manzaki section, which has a thickness of 3,950 m, Qayyum et al. (1996) conducted a classification of the Shaigalu component, dividing it into three distinct components. The upper portion comprises a sandstone sequence with a thickness of 591 meters. This sequence exhibits characteristics such as thick to extremely thick bedding, ripple lamination, cross-bedding, and sandblasting, resulting in the formation of colorful mudstone. In contrast, mudstone exhibits the presence of sandstone lenses, siltstone, layers of soil, and coal beds. The center part of this component is 698 m in thickness and is characterized by numerous fining-upward cycles. These cycles consist of trough to planar cross-bedded sandstone, which is interbedded with greenish grey to chocolate brown mudstone and siltstone exhibiting severe bioturbation. In a similar vein, the lower portion of the Shaigalu component exhibits a thickness of 661 m and is composed of sandstone with distinct bedding, accompanied by laminated greenish grey siltstone and shale. These sedimentary layers are characterized by a flat to mixed configuration, as well as hummocky cross bedding.

The deposition of members from the Shaigalu and Murgha Faqirzai formations occurred within a river delta system that had been changed by wave action, as shown by

Qayyum et al. in 1996. The Hunting Survey Corporation (1960) assigned an Oligocene age to the Shaigalu member, but the upper contact of this member is not visible inside the study site.

### **2.2.5 Dasht Murgha Group**

The stratigraphic unit in question is observed in the Dasht Murgha region, encompassing a wide and expansive syncline that extends from Muslim Bagh to Naweoba, in close proximity to Zhob. The Khojak formation was initially delineated by the Hunting Survey Corporation in 1960. In their studies, Qayyum et al. (1997a, 2001) shown that the Bostan formation and Murgha group can be considered as a unified entity, referred to as the Sharankar formation. In the Naweoba region, the group attains its maximum thickness of 4800 meters. The lithological properties of this group lead to its further subdivision into the Khuzhobi, Bahlol Nika, and Sara Khula formations. The Khuzhobi formation comprises a cyclic succession of sandstone and mudstone. Similarly, the Bahlol Nika formation consists of a thick succession of sandstone interbedded with mudstone. On the other hand, the Sra Khula formation is characterized by a cyclic alteration of mudstone, sandstone, and siltstone. The classification of this group is within Zone III.

### **2.2.6 Malthanai Formation**

The Malthanai formation was designated by the Hunting Survey Corporation (1960) in reference to the Malthanai village inside its stratigraphic section. The aforementioned formation is observed in proximity to the Nisai formation or the Dasht Murgha group in the regions of Kazha Merzai, Garda Manda, Malthanai Killi (in close proximity to the type section), and Sur Kach. Based on the findings of the Hunting Survey Corporation (1961), the formation in question exhibits a connection to the Shaigalu and Murgha Faqirzai members, and may be identified as a conglomeratic axial belt facies associated with these members. The thickness of this structure measures 2500 meters. The geological formation under consideration is classified as zone IV, characterized by a predominant composition of sandstone that is interspersed with layers of siltstone, mudstone, and conglomerate. Further clarification is required with respect to the depositional environment.

### **2.2.7 Bostan Formation**

The nomenclature "Bostan formation" was designated by the Hunting Survey Corporation (1960) in reference to the hamlet of Bostan, situated around 30 kilometers north of Quetta. The designated classification of this particular area is referred to as Pishin Lora, which is within the jurisdiction of the Pishin district. The Bostan formation predominantly consists of red mudstone, accompanied by lesser quantities of sandstone and conglomerate. The geological structure found in the Zhob valley consists of alternating layers of conglomerate, mudstone, and sandstone. These layers can attain a maximum thickness of 1250 m in the Gardab Manda area located to the north of Killa Saifullah.

### **2.2.8 Zhob valley deposits**

The deposits found in the Zhob valley are characterized by their substantial thickness and extensive coverage across a significant portion of the valley. The composition of these formations mostly consists of mudstone, which is interspersed with sandstone, siltstone, and pebbly conglomerate. The aforementioned deposits exhibit a high degree of porosity and fragility. The flat and loose form of the subject under discussion can be attributed to its Holocene nature, as noted by Kasi et al. (2012).

## **2.3 Muslim Bagh Ophiolite**

The suture belt, located between the Afghan Block and the Indian plate, undergoes thrusting over the calcareous belt (Sengor, 1987). The suture band is composed of the Muslim Bagh and Khanozai ophiolite complexes. The Muslim Bagh ophiolite was initially characterized by Otsuki et al. (1989) as a distinct geological formation located between the flysch zone and the calcareous belt. The Muslim Bagh ophiolite, situated in the southeastern region of the Muslim Bagh village/town, has two substantial massifs. According to Bilgrami (1964), the Jang Tor Ghar Massif is situated to the west, while the Saplai Tor Ghar Massif is located to the east. The Jang Tor Ghar Massif, characterized by a summit elevation of 3010 meters and a land area spanning 150 square kilometers, primarily consists of foliated peridotite. The geographical expanse included by Saplai Tor Ghar spans over 600 square kilometers, featuring a maximum altitude of 2700 meters. The Saplai Tor Ghar Massif exhibits a remarkable resemblance to a genuine ophiolitic sequence, making it the

most noteworthy among them. The Massif in question comprises a sequence of foliated peridotites, transition zone rocks, and crustal rocks, arranged in a vertical succession. Numerous outcrops containing a significant amount of dunite in the surrounding area have been subjected to mining activities for the extraction of chromite. The Muslim Bagh region exhibits an impressive assemblage of mafic dykes within the Ophiolitic series, which are visually striking and can potentially be observed from aerial perspectives. The observed dykes exhibit a thickness ranging from 3 to 5 meters and are composed of mafic rock. The researchers made incisions in the highest ophiolitic sequence. The Saplai Tor Ghar Massif is the sole geographical region where the Earth's crust is observable. The basal section of the Saplai Tor Ghar Massif is comprised of cumulate dunite, wherlite, and pyroxenite, overlain by stratified and foliated gabbro. The geological investigation conducted in the Muslim Bagh region revealed that the formation of sheeted dykes, gabbros, and mafic dykes can be attributed to the process of supra-subduction, as documented by Kakar (2011) and Khan et al. (2007).

#### **2.4 The ultramafic rocks north of Muslim Bagh (Shina Khwara)**

The highly tectonized ultramafic rocks of Shina Khwara are strikingly different from their southern counterparts. Their position suggests that the allochthonous masses of the south Muslim Bagh complex may have originated from this northern belt (Farah and DeJong, 1979).

The ultramafic rocks occur as a light gray green, highly sheared mass, rich in disseminated talc and with some asbestos. They form a typically smooth, rounded topography in contrast to the otherwise rough forms of the Muslim Bagh masses. More normal ultramafic lenses are preserved only along the upper, northern contact, or together with the rather widespread rodingites. All contacts are tectonic. To the south, north-dipping sandstones and reddish siltstones of Miocene age are steeply, and partly discordantly, overthrust by the sheared ultramafic rocks. The thrust zone dips northward. The upper, northern thrust is much flatter and exposes, along the thrust zone, boudinaged and serpentized harzburgites, which locally contain some apparently iron-rich chromite. Above the ultramafic rocks are thick lenticular nummulitic limestones and a well-bedded sequence of shales and limestones of Eocene age. Locally the contact can be steeper, well

exposed in the creek at the western extension of the outcrops, coinciding with a sulfurous spring. Some of the Eocene cover is disharmonically folded and faulted, and these structures seem to predate the final thrusting. This thrusting, particularly the relatively flat thrust of the Eocene, might have covered a considerable part of the ultramafic mass which may therefore extend further to the north (Farah and DeJong, 1979).

Based on the few observations made during the reconnaissance trip, there must be stress on the importance of investigating the Shina Khwara mass in more detail, both geologically and geophysically. The connection of this mass with the main Muslim Bagh bodies below the Tertiary and Quaternary cover may give some hints on the structural origin of the latter. The Muslim Bagh ultra-mafic masses must have been transported southward as detached blocks, since some of the primary structures (original banding and dike intrusions) are preserved, although they are overprinted by later tectonics. In contrast, the primary structures of the Shina Khwara masses have been obliterated, and the present configuration even suggests some very late diapiric emplacement subsequent to intense tectonic compression. It could be that this belt represents a kind of "root zone" to the allochthonous Muslim Bagh tectonic sheets, and that it follows the actual Suture Zone. The northern extension below the Eocene thrust is therefore probably not large (Farah and DeJong, 1979).

The allochthonous position of the large Muslim Bagh ultramafic masses is generally accepted by modern investigators. One may even suggest that these masses are thrust over locally preserved melange zones and flyschoid sediments in a way similar to the classic occurrences in the Central Himalayas (Gansser, 1974).



## **CHAPTER 03**

# **MAGNETIC DATA ACQUISITION AND PROCESSING**

### 3.1 Introduction

Geophysics can be termed as a science that applies physical and mathematical methods for subsurface studies. It is dependent on the aims and purposes of the parameter estimation research with the aim of magnetic survey to detect and describe parts of the Earth's crust with abnormal magnetizations (Joshua et al., 2017).

- Magnetic surveying consists of the following:
- At predefined sites, the terrestrial magnetic field is measured.
- Adjusting measurements to account for diurnal variations.
- Comparison of resultant values of field with expected value at each measurement station.
- Calculation of the estimated depths from Earth's surface to magnetic magnetic anomaly source.

Nwankwo et al. (2007) state that the presence of iron and nickel in some minerals gives rise to ferromagnetic properties. Consequently, rocks containing these metals possess notable magnetization and generate localized magnetic fields. The utilization of non-destructive technology is prevalent in geo-environmental investigations, encompassing several applications such as the identification of voids, near-surface faults, igneous dikes, and subsurface ferromagnetic objects (Weymouth, 1986). The utilization of magnetic field fluctuations enables the determination of anomaly depth, geometries, and magnetic susceptibility. According to Joshua et al. (2017), the utilization of magnetic anomaly maps is valuable in facilitating geological interpretations.

The International Geomagnetic Reference Field (IGRF) is widely recognized as the theoretical representation of the magnetic field's undisturbed state at any given location on the Earth's surface. The aforementioned formula is employed to eliminate magnetic deviations that can be attributed to the theoretical field, resulting in residual magnetic anomaly data. Consequently, a magnetic anomaly can be defined as the discrepancy between the measured magnetic field of the Earth and the anticipated magnetic field derived from the International Geomagnetic Reference Field (Lowrie, 2020). There is an alternate method available for conducting short surveys, in which the regional field is estimated as a

linear trend and subsequently removed from the final field value at each measurement location. The name "trend analysis" refers to this approach (Kearey et al., 2002).

### 3.2 Survey Planning

Preliminary planning is essential for any geophysical work to facilitate field operations and settle any other issues that may happen during the survey. The main objective of the planning is not only to save time and money, but also to increase data quality and obtain as much information as possible. Consideration in the sequence of surveying pattern, data collection, and processing procedure provide us with an opportunity to enhance data signal-to-noise ratio, which is ultimately vital in the final interpretation of any geophysical survey.

### 3.3 Data Acquisition in Semi-Detailed Survey

Ground data acquisition was performed with the help of Proton Precision Magnetometer (Geometrics 856-AX). Data was observed at approximately 300 to 500 meters spacing along Quetta-Zhob highway, all fair-weather motor-able tracks, paths along Nalas and even on foot when it thought to be necessary. About 1012 magnetic stations were observed during semi detailed magnetic survey. Figure 3.1 below displays survey points.

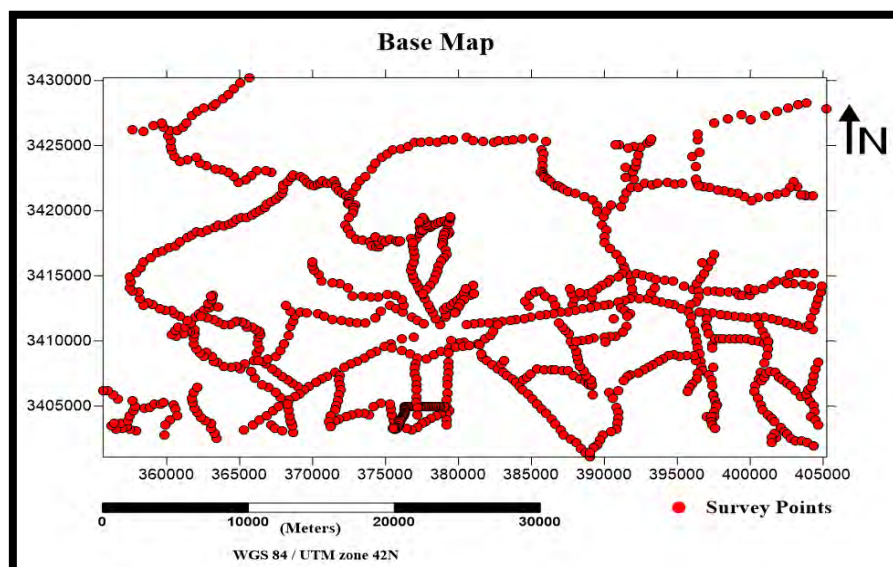


**Figure 3.1:** Magnetic data acquisition base map of study area showing survey points along various profiles in the study area.

## 3.4 INSTRUMENTS USED

The following instruments were used in magnetic data acquisition.

### 3.4.1 Magnetometer

The G-856AX provides a reliable, cost-effective solution for a variety of magnetic mapping applications. The G-856AX uses the well proven proton precession technology. The G-856AX makes a hydrogen rich fluid (like kerosene) surrounded by an induction coil to generate a strong magnetic field. Subsequently, the spin axis of the hydrogen protons polarizes with the newly applied magnetic field.

Protons begin to align themselves along the Earth's magnetic field at particular frequency (proportional to surrounding magnetic field intensity) after the current causing the polarizing field is interrupted (Lenz, 1990).

This precession phenomena induces an alternating current in the induction coil which was previously being used for the generation of the polarization field (Lenz, 1990). The factor relating to the precession frequency of the induced voltage with the earth's magnetic field strength is termed proton gyro-magnetic ratio and has a value of 0.042576 Hz/nT. The G-856 magnetometer can be used as a gradiometer with two sensors, or for automatic value recording at the base station (Jeng et al., 2003). Its storage capacity reaches up to 5000 observations with single sensor and 2500 with two sensors. G-856 portable man conveyed proton precession magnetometer of Geometrics was utilized to observe the magnetic intensity at the observation stations as well as at the base station (Fig. 3.2).

It gives a precise value of up to 0.1 gamma in normal conditions and 1 gamma in case of supreme conditions. It has a gradient tolerance of 1800 gammas/meter. The instrument was calibrated at the established base station by setting its clock, inputting the Julian date, and tuning the instrument in accordance with the regional magnetic field from the international standard Total Magnetic Intensity map. The software used for the data transfer and editing is MagMap2000.



**Figure 3.2:** G-856AX Geometrics Proton Precision Magnetometer used for magnetic data acquisition.

### 3.4.2 Hand-held GPS

Garmin Oregon 450 and Garmin e-Trex GPS, Global Positioning System has been used to determine locations of stations shown in Figure (3.3)



**Figure 3.3:** Garmin hand-held GPS used to determine the coordinates of the observation stations.

## **3.5 Acquisition Parameters**

The data collecting process involved the utilization of Geometrics G-856AX, Proton Precision Magnetometers, which possess a resolution of 0.001 nT and a cycle rate of 0.1 second. The observed noise envelope had an average magnitude of less than +/- 0.02nT. The Garmin GPS etrex 10 and Garmin Oregon 450 Handheld GPS devices were employed to determine spatial coordinates in both the Universal Transverse Mercator (UTM) and Latitude-Longitude systems. The magnetometer was calibrated to a value of 48000 nT using the global magnetic map.

### **3.5.1 Recording Parameters**

Data recording methods will vary with the purpose of the survey and the amount of noise present. Ground magnetic measurements made at regular intervals from 300-500 meters along profiles. Variations of intervals made based on magnetic observations during acquisition. sensor heights of up to 2 m have been used to remove near-surface effects.

## **3.6 Precautions**

The following precautions are necessary before recording the magnetic readings.

- Man-made electromagnetic sources can affect magnetic results during operations of survey. Steel and other ferrous metals near a magnetometer can distort the data.
- It is necessary to remove large belt buckles and other similar accessories while running the equipment.
- One conclusive examination involves the immobilization of the magnetometer, followed by the collection of readings as the operator traverses the vicinity of the sensor. If the readings exhibit a variation of no more than 1 or 2 nanotesla (nT). In order to ensure the accuracy of highly accurate surveys, it is imperative to maintain the operator effect at a level below 1 nT.
- In order to acquire a reliable and accurate reading, it is imperative to operate the sensor at a considerable distance from the ground. The aforementioned technique is conducted due to the likelihood of soil magnetite aggregations causing interference with ground-level readings. In areas characterized by rugged topography, the

presence of rocks containing a certain proportion of magnetite can provide a potential source of error in accurately measuring the magnetic properties of the underlying subsoil.

- Nearby metal objects may cause interference.
- Old, buried curbs and foundations, buried cans and bottles, power lines, fences, and other hidden factors can greatly affect magnetic readings.

## **3.7 Magnetic Data processing**

### **3.7.1 Introduction**

Similar to the gravity method, magnetic measurements encompass the effects of various factors, such as topography, natural and human-induced surface characteristics, as well as instrumental, geological, and planetary influences. The sources presented exhibit a wide array of amplitudes and durations in relation to temporal fluctuations, as well as spatial contributions in terms of wavelengths. The qualities indicated above have the ability to obscure or alter the magnetic phenomena originating from subsurface sources that are important in the survey (Hinze et al., 2013). Consequently, the collected data is analyzed with the objective of alleviating or reducing these effects. The outcome of this particular processing procedure yields the magnetic anomaly. Fortunately, in the majority of magnetic survey campaigns, the impact of these additional factors on distorting the impacts of subsurface sources is significantly less pronounced when compared to the gravity approach. Therefore, the magnetic methodology exhibits fewer rigorous constraints on auxiliary data and reduction techniques when compared to the gravity method. The alterations pertaining to these impacts are primarily ascertained using experimental methodologies, wherein observations are made regarding the temporal and spatial attributes of magnetic fields (Hinze et al., 2013).

During magnetic data processing the following corrections were applied to magnetic data.

### **3.7.2 Diurnal variation**

The Geomagnetic field fluctuates within short periods of time of the order of hours due to the movement of charged particles in the ionosphere. These variations are called

diurnal variations and to correct for these variations, diurnal-correction was applied by reoccupying the base station (Dentith and Mudge, 2014).

Diurnal variation normally has a daily period and an amplitude averaging about gammas. This sometimes can reach an amplitude of 100 gammas; thus, they must be considered to make safe the signal from such noisy effects. The utilization of diurnal variations, as in this instance, demands the simultaneous employment of two magnetometers, one at the base station and one in the field area. Following the same procedure, one device was permanently installed at the base station, which recorded continuous fluctuations every 10 minutes. The data from the base station was plotted against time to show the behavior of the diurnal variation about the base station.

These continuous base station measurements observed in the vicinity normally suggest that the external field's behavior was fairly smooth. In applying the diurnal correction, the first step was to link the measurements to a certain zero time at a defined reference.

Each field measurement was timed, and the measured difference in intensity was adjusted by adding or subtracting the departing amount noted from the base curve at the time of field measurements.

### **3.7.3 Normal Correction**

Since the geomagnetic field is a bi-polar field, therefore the magnetic field also fluctuates in the north south and east-west direction, i.e., as we move from equator to poles, the field increases. Therefore, to account for this variation, normal-correction is applied; a value of 4.0 nano Tesla/km along N-S direction and 1.0 nano Tesla /Km was used for this purpose (Dentith and Mudge, 2014).

### **3.7.4 Reduction to Equator**

The procedure entails mitigating the reliance of magnetic data on the Earth's magnetic inclination. The process involves converting data that was originally measured inside the inclined magnetic field of the Earth to its hypothetical values on the assumption that the magnetic field was vertically aligned (Ganiyu et al., 2013). This method improves



the process of interpretation by transforming the irregular responses of sub-vertical prisms or sub-vertical contacts (including faults) into more easily understandable symmetric and antisymmetric patterns.

The symmetric "highs" exhibit a fine alignment with the center of the geological body, but the greatest gradient of the antisymmetric dipolar anomalies demonstrates a perfect correspondence with the limits of the body. This approach has significant importance in the context of magnetic data gathered at low latitudes. Within the designated research region, the land magnetic data were subjected to a procedure often referred to as Reduction to the equator (RTE) (Ganiyu et al., 2013).

### 3.7.5 Upward Continuation

Upward continuation is a mathematical method used to extrapolate data collected at a certain elevation to a higher elevation. This process results in the smoothing out of short-wavelength features because the data is being shifted away from the original anomaly. Essentially, upward continuation is employed to highlight and emphasize large-scale features, typically those found at greater depths in the surveyed area. It achieves this by reducing the influence of anomalies with shorter wavelengths, as they are attenuated more. Additionally, this technique tends to magnify anomalies originating from deeper sources while diminishing those originating from shallower sources (Mekonnen, 2004).

The upward continued  $\Delta F$  (the total field magnetic anomaly) at higher level ( $z = -h$ ) is given by,

$$\Delta F(x, y, -h) = \frac{h}{2\pi} \iint \frac{\Delta F(x, y, 0) dx dy}{((x - x_0)^2 + (y - y_0)^2 + h^2)^{\frac{3}{2}}} \quad (1)$$

Therefore, the procedure of numerically integrating surface data in order to ascertain the field at a higher level using lower-level information is quite uncomplicated. In practical applications, the aforementioned computations are executed by replacing the surface integral with a weighted summation of data derived from a standardized grid. The empirical formula, which was first proposed by Henderson in 1960, is used for the purpose of computing the field strength at a certain elevation, referred to as 'h,' above the reference

field plane ( $z = 0$ ). This field is characterized in terms of the average value  $\Delta F(r_i)$  across a circular area centered at coordinates  $(x, y, 0)$  with a radius of  $r_i$ . The formula comprises weighting factors that are appropriately assigned to allow for essential changes. According to Sharma's findings in 1985, the use of these factors allows for a high degree of accuracy, namely 2%, in the computation of the upward continuing field.

### **3.7.6 First Order Vertical Derivative**

This methodology reveals best productivity when addressing shallow source depths and rock formations characterized by significant disparities in magnetism. In sedimentary environments, where the rocks possess a low level of magnetization, even notable structures may have a mild magnetic signature. Consequently, the use of filtering techniques to enhance these weak anomalies is a crucial aspect of the interpretation process. The use of vertical derivatives in potential field analysis is advantageous as it serves to reduce the lateral extent of anomalies, hence enhancing the accuracy of source body identification. The amplification of the impact becomes more pronounced as the order of the derivative used increases. Nevertheless, it is important to note that derivative filters, being a kind of high pass filter, also amplify noise in the data to the same extent (Cooper and Cowan, 2004).

### **3.7.7 Horizontal Derivative**

Filtering magnetic data and performing image processing on it are both crucial processes in mineral prospecting. When dealing with shallow source depths and rock types with relatively large differences in magnetism, this approach is at its most effective. The horizontal derivative of the potential field has practical applications since it improves the edges' contact with anomalous bodies (Cooper and Cowan, 2004).

## **CHAPTER 04**

# **INTERPRETATION AND ANALYSIS OF MAGNETIC DATA**

## 4.1 Introduction

The analysis of magnetic readings bears a resemblance to the interpretation of gravity measurements. However, there are notable differences. An illustration of this can be seen in the utilization of the magnetic technique, which relies on a dipolar field as opposed to a monopolar gravity field. Consequently, magnetic signals encompass the combined effects of attractive and repulsive forces, thereby posing challenges in their interpretation. Nevertheless, due to the dipole nature of the magnetic field, magnetic anomalies exhibit a higher degree of sensitivity to depth compared to gravity anomalies.

In addition, the focus of gravity measurements primarily lies in the examination of variations in the vertical component. Conversely, the magnetic method offers a diverse array of measurements for analysis, encompassing the standard total field anomaly as the typical scenario, as well as vector, gradient, and tensor components acquired through suitably positioned sensors on land, as well as on ships, aircraft, and satellites. Magnetic measurements are commonly acquired by the utilization of parallel rails. Consequently, the data can be visually represented and comprehended either in the form of profiles or as a two-dimensional map delineating isoanomaly contours. Both profile and map interpretations possess unique advantages and limitations. The information is depicted in a cartographic representation that emphasizes the two-dimensional spatial arrangement of anomalies. Nevertheless, due to its nature as a high-cut filtering technique, contouring tends to result in the loss or reduction of low-amplitude, higher-frequency anomalies in anomaly maps. In order to mitigate this concern and prioritize the examination of gradients, which hold significant importance in the process of interpretation, it is common practice to present and analyze data in the form of profiles (Hinze et al., 2013).

Interpretation consists of two types, namely qualitative and quantitative, with the meaning of the terms explained as follows:

- The qualitative data interpretation strategy is utilized to examine qualitative data, which is otherwise called all out information.
- The quantitative information interpretation technique is applied to analyze quantitative information, which is otherwise called mathematical information.

- This sort of information contains numbers and is accordingly studied with the utilization of numbers.

## **4.2 Qualitative Interpretation**

The reduced magnetic data were processed further in Surfer-20 software to generate magnetic anomaly maps, total magnetic intensity (TMI) maps and anomalous zone map of study area in this software. First of all, coordinate system of data was set in the software. It was in geographical coordinate system and was converted into projected coordinate system by using reference WGS84 datum. The study area falls in zone 42 north.

## **4.3 Gridding**

After setting up the coordinates of data, grids were prepared by applying different filters. The appropriate technique which was utilized for the production of grids was minimum curvature.

## **4.4 Division of Data**

In the initial phase of data interpretation, two comprehensive toposheets (34N/9 and 34N/13) are utilized to visually represent and analyze anomalous zones. These aforementioned toposheets are individually evaluated for further analysis.

## **4.5 Semi-Detailed Magnetic Data Interpretation of Toposheet 34N/9**

The present topographic map encompasses the central urban region of Muslim Bagh. The profiles were obtained using a magnetic observation point interval ranging from 300 meters to 500 meters. The profiles were conducted in an east-west direction along the highway and foothills. Subsequently, the majority of profiles were conducted in a north-south direction, traversing the mountain ranges in order to achieve comprehensive coverage of the surveyed area. The majority of the topographic sheet comprises mountain ranges situated at high altitudes.

#### 4.5.1 Magnetic Anomaly Map of Toposheet No. 34N/9

The magnetic anomaly map of the magnetic data from toposheet 34N/9 was generated using the minimum curvature technique in Surfer-20 software. The map is depicted in Figure 4.1, with a contour interval of 50 nT. The high anomalous zone exhibits a transition in color from green to pink, with a range of values between 450 nT and 2550 nT. The presence of a magnetic body in the subsurface is closely linked to the occurrence of this elevated anomalous zone. The low anomalous zone is visually indicated by the color blue, with a corresponding range of values spanning from -150 nT to -600 nT. The presence of a low anomalous zone indicates the absence of magnetic properties in the subsurface region. The dominant hue of light blue depicted on the map signifies the range of magnetic anomaly values, spanning from -150 nT to 300 nT, which indicates the existence of sedimentary rocks within the designated study area.

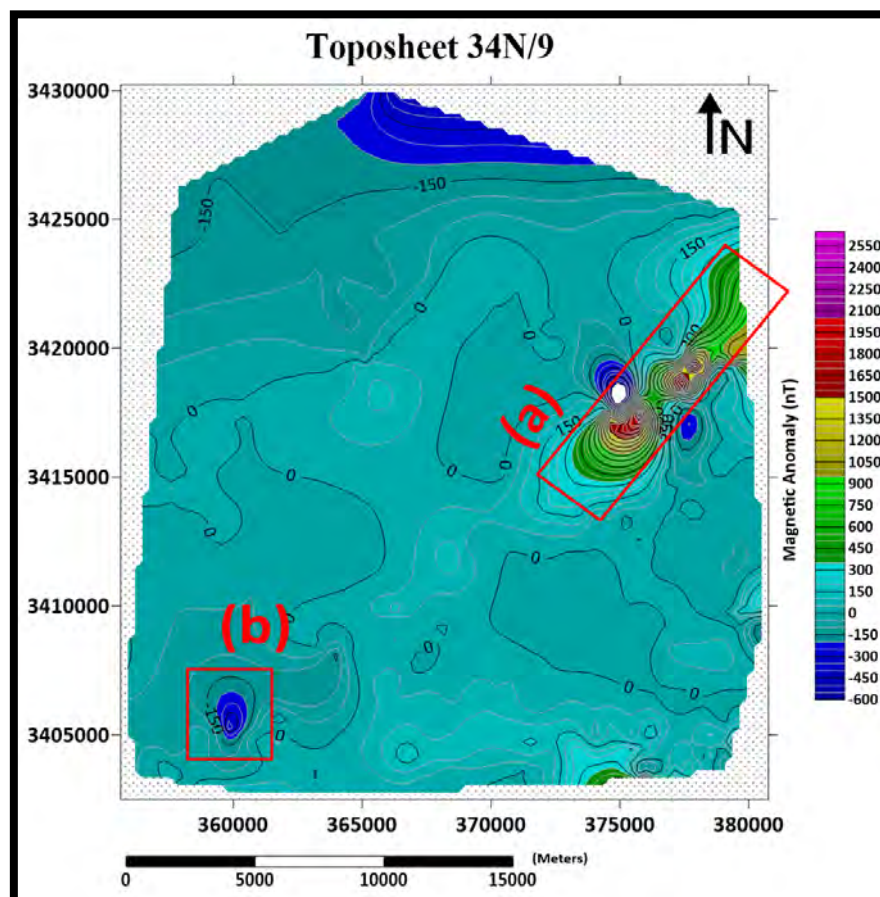


**Figure 4.1:** Magnetic anomaly map of toposheet 34N/9 showing high and low magnetic anomalous zones with rectangles (a) & (b) respectively.

#### 4.5.2 Total Magnetic Intensity (TMI) Map of Toposheet No. 34N/9

The magnetic data from toposheet 34N/9 have been utilized to create a total magnetic intensity (TMI) map, as shown in Figure 4.2. The contour interval used for plotting is 50 nT. The total magnetic intensity map exhibits a range spanning from 47200 nT to 50500 nT, within which it is capable of effectively discerning a high magnetic zone characterized by values ranging from 48400 nT to 50500 nT. The area under consideration has a low magnetic zone characterized by magnetic values ranging from 47200 nT to 47800 nT. Therefore, the topographic map 34N/9 provides confirmation of the presence of both high and low magnetic anomalous zones as indicated in the magnetic anomaly map depicted in figure 4.1.

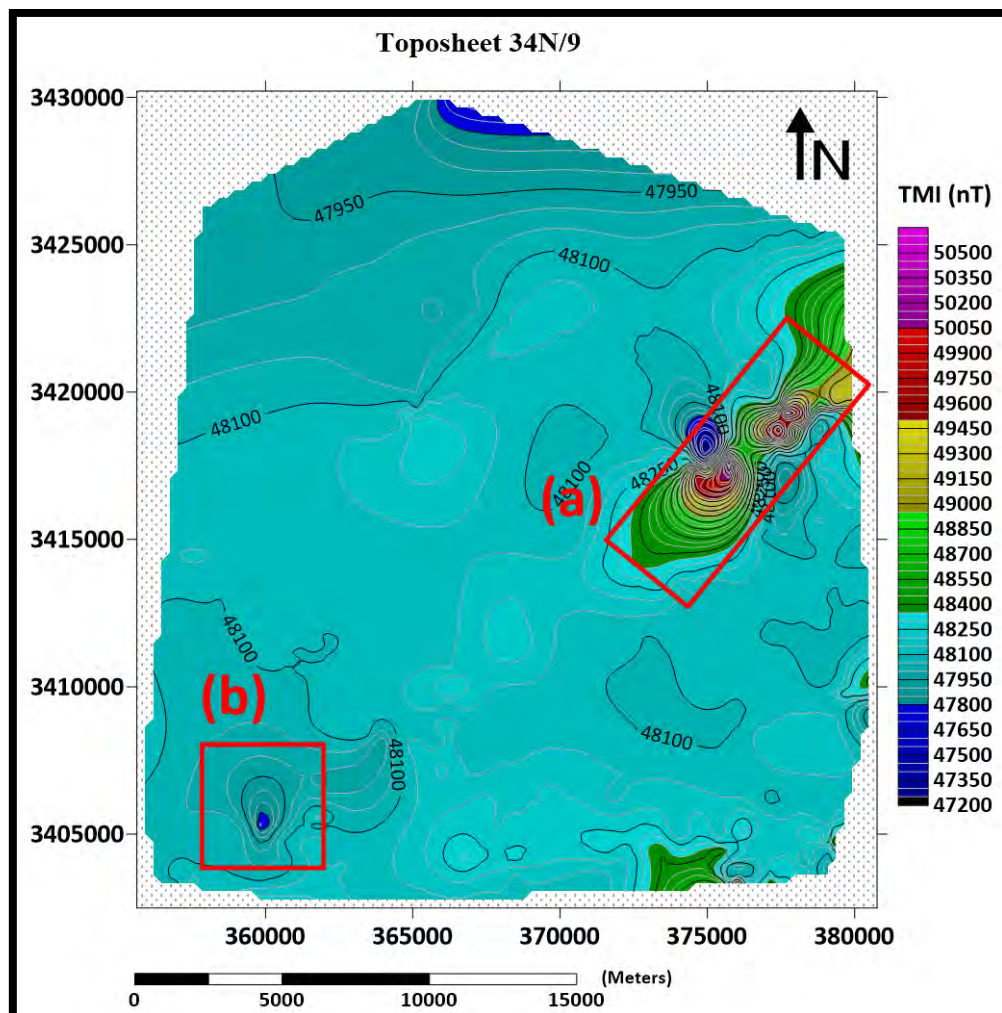


Figure 4.2: Total Magnetic Intensity (TMI) map of toposheet 34N/9 showing high and low magnetic zones with rectangles (a) & (b) respectively.

## 4.6 Semi-Detailed Magnetic Data Interpretation of Toposheet 34N/13

The majority of this topographic sheet comprises a region characterized by elevated terrain, primarily located in the southern vicinity of Muslim Bagh. The data were obtained using a profile interval ranging from 2.5 kilometers to 4 kilometers. The profiles were initially surveyed in an East-West orientation, following the highway and foothills. Subsequently, the majority of profiles were surveyed in a North-South direction, traversing the mountain ranges, in order to achieve comprehensive mapping coverage of the entire sheet.

### 4.6.1 Magnetic Anomaly Map of Toposheet No. 34N/13

The anomaly map of toposheet 34N/13 has been generated using Surfer-20 software. The contour interval used is 50 nT, and the minimum curvature technique was employed to create the map, as depicted in Figure 4.3.

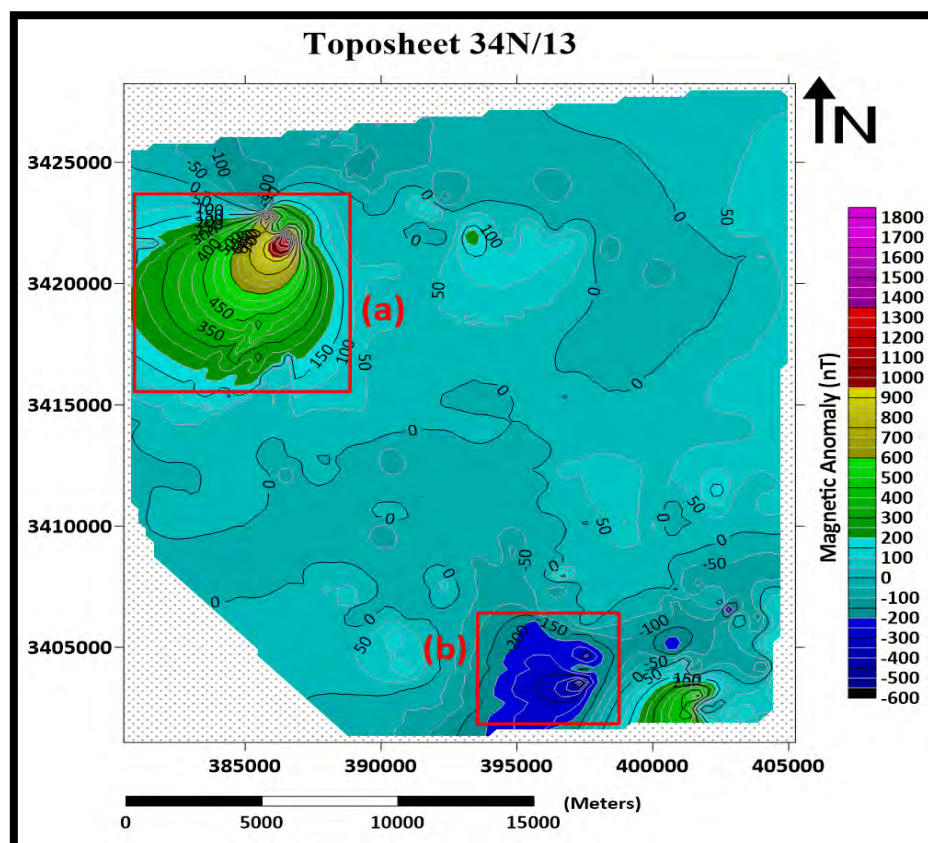


**Figure 4.3:** Magnetic anomaly map of toposheet 34N/13 depicting high and low anomalous zones marked with rectangles (a) & (b) respectively.



The magnetic anomaly map indicates the presence of two notable anomalous zones. The presence of elevated magnetic anomalies in a certain area is denoted as a high anomalous zone, which is visually emphasized by a rectangular shape labeled as (a). The magnetic anomaly measurements span a range of 300 nT to 1800 nT. Another region, denoted by rectangle (b), exhibits a low level of anomalies. The low anomalous zone is characterized by magnetic anomaly values ranging from -50 nT to -600 nT. The high magnetic anomalous zone is situated in the northwestern direction of the toposheet, whereas the low magnetic anomalous zone is predominantly concentrated in the southern region.

#### 4.6.2 Total Magnetic Intensity (TMI) Map of Toposheet No. 34N/13

TMI map is generated to depict areas of high and low magnetic intensity within the designated study region. The TMI map of toposheet 34N/13 was generated using the minimum curvature technique, employing a contour interval of 50 nT. The TMI map (Figure 4.4) indicates the presence of two distinct magnetic zones.

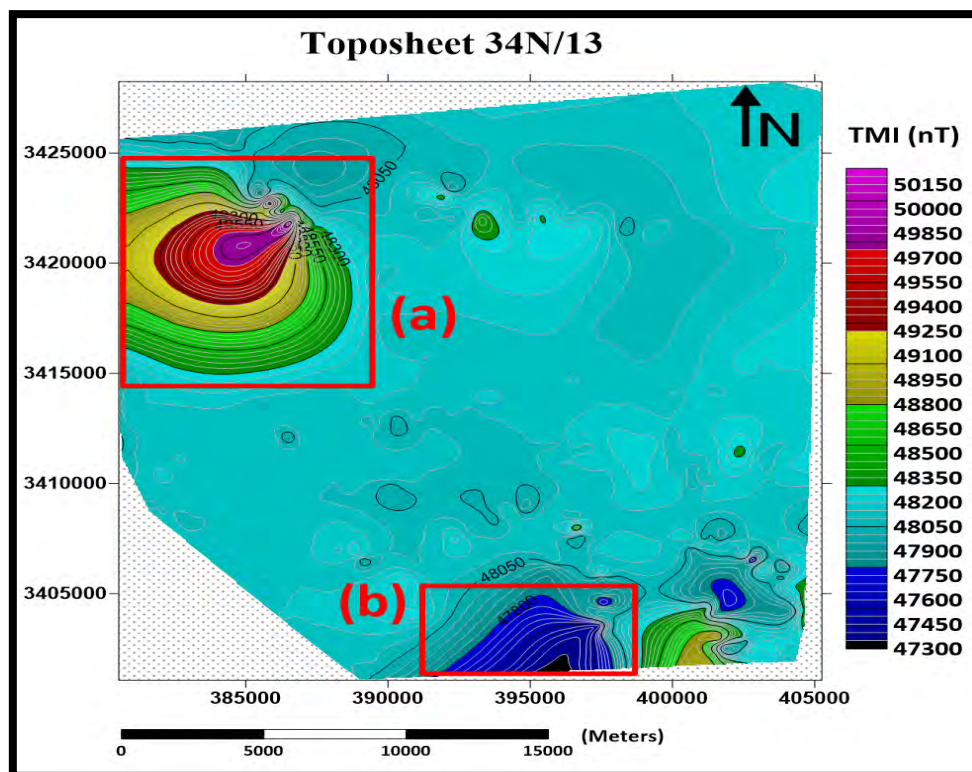


**Figure 4.4:** Total Magnetic Intensity (TMI) map of toposheet 34N/13 depicting high and low magnetic zones marked with rectangles (a) & (b) respectively.

One particular area has a strong magnetic field, characterized by a range of Total Magnetic Intensity (TMI) values spanning from 48350 nanoteslas (nT) to 50150 nT. The range of values for the low magnetic zone spans from 47300 nT to 47900 nT. The primary objective of the TMI map is to validate the presence of anomalous areas as indicated in the magnetic anomaly map of toposheet 34N/13. The TMI map exhibits regions of elevated and diminished magnetic intensity, denoted by rectangles (a) and (b) correspondingly.

#### 4.7 Semi-Detailed Magnetic Data Interpretation of Combined Toposheets (34N/9 & 34N/13)

The two toposheets, namely 34N/9 and 34N/13, were combined in order to observe the uninterrupted magnetic, geological, and geometrical characteristics of the designated study area, as depicted in Figure 4.5.

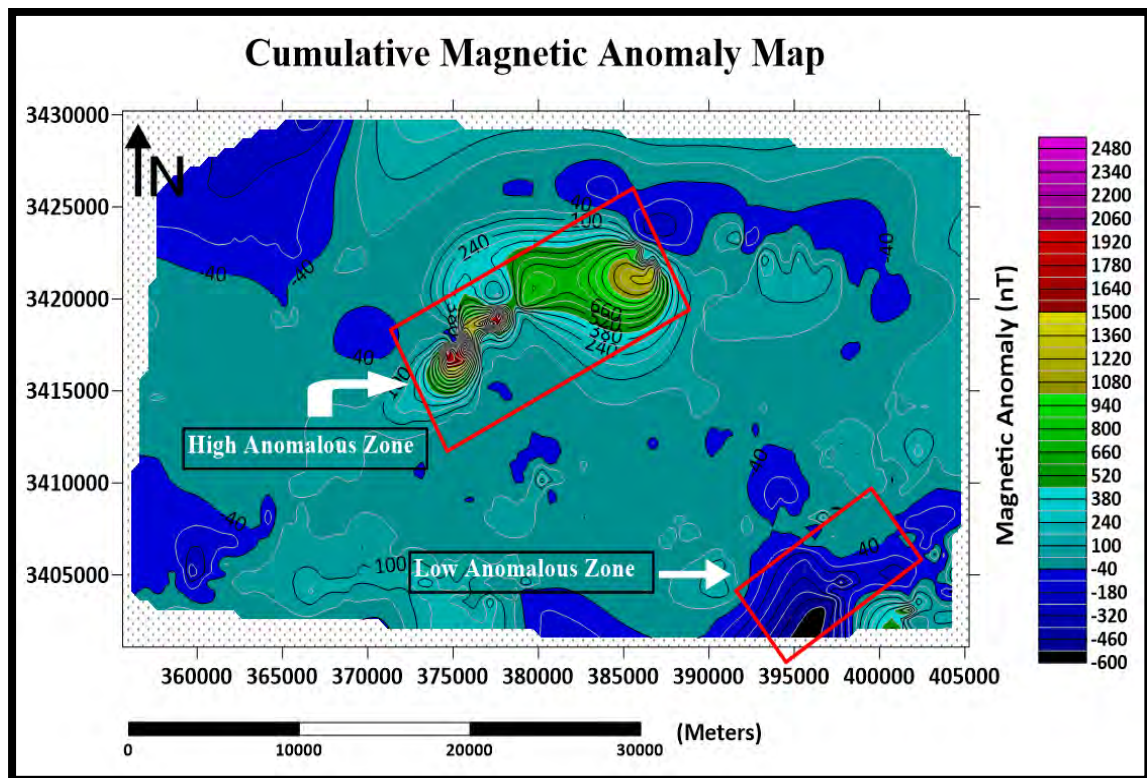


**Figure 4.5:** Cumulative magnetic anomaly presentation of toposheets (34N/9 & 34N/13) highlighting high and low anomalous zones with arrows.

The analysis of magnetic data has unveiled the presence of a higher magnetic anomalous zone with a southwest to northeast trend. The anomalous zone exhibits a

spectrum of magnetic values spanning from 520 nanotesla to 2480 nT. The lower magnetic anomalous zone exhibits magnetic anomaly values that span from -40 nT to -600 nT. The research area contains a southern region characterized by a low anomalous zone. The studied area exhibits a correlation between elevated magnetic anomalies and the presence of magnetized material within the subsurface. Lower magnetic anomalies are typically observed in subsurface materials that exhibit nonmagnetic properties. In order to achieve a more accurate and precise interpretation of the research region, it is imperative to map these anomalous zones by employing comprehensive magnetic and other geophysical techniques.

#### 4.8 Cumulative Total Magnetic Intensity (TMI) Map

The minimum curvature technique was employed to generate a cumulative total magnetic intensity map of the toposheets (34N/9 & 34N/13). The contour interval used in the map was set at 80 nT, as depicted in Figure 4.6. The studied region exhibits two distinct zones of prominence. A region is characterized by high levels of magnetic intensity, and this region has a directional tendency from the southwest to northeast. The region char-

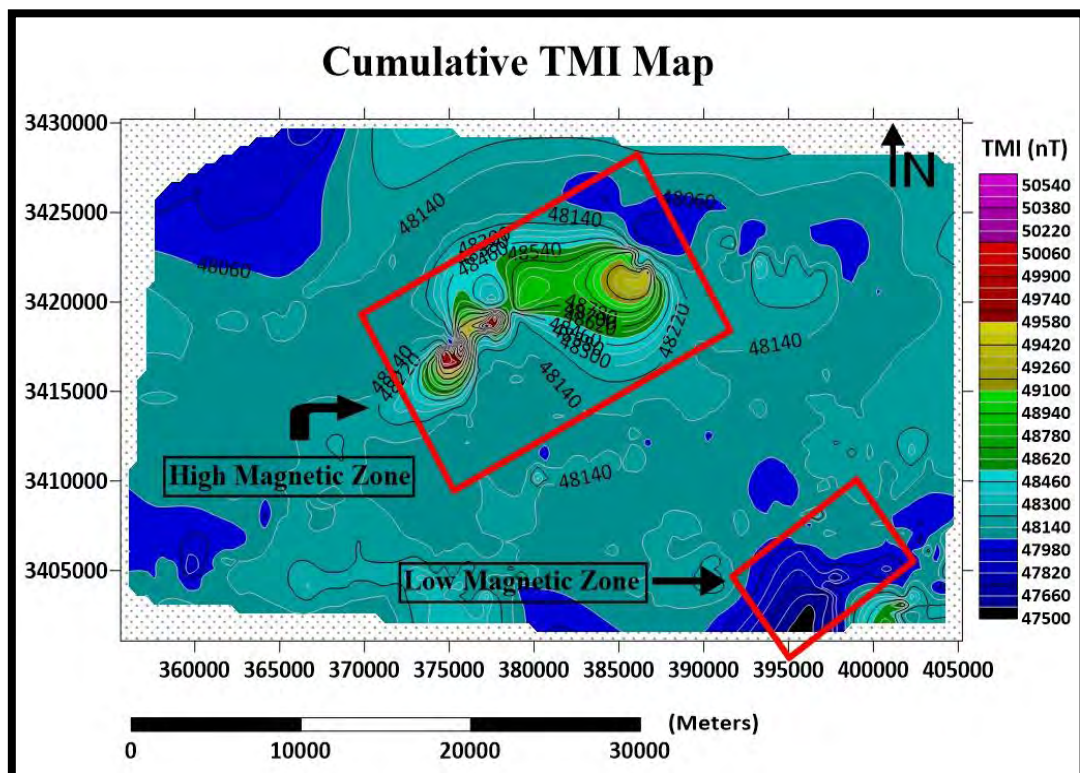


**Figure 4.6:** Cumulative total magnetic intensity (TMI) display of toposheets (34N/9 & 34N/13) indicating high and low magnetic zones with rectangles as described in the figure.

acterized by intense magnetization is visually depicted by a color spectrum ranging from green to pink. The total magnetic intensity (TMI) values within the high magnetic zone exhibit a range of 48620 nT to 50540 nT. An other region exhibits diminished levels of magnetic intensity. The observed values span a range of 47500 nT to 47980 nT, with the corresponding color gradient representing this zone as ranging from dark blue to black. The correlation between increased magnetic intensity and magnetic behavior of the subsurface in the research area is evident. Lower magnetic intensities are indicative of nonmagnetic characteristics inside the subsurface.

#### 4.9 3D Visualization of Cumulative Anomaly Map

The 3D visualization of cumulative magnetic anomaly data for both toposheets serves to depict the fluctuations in the form of magnetic highs and lows, as illustrated in Figure 4.7.

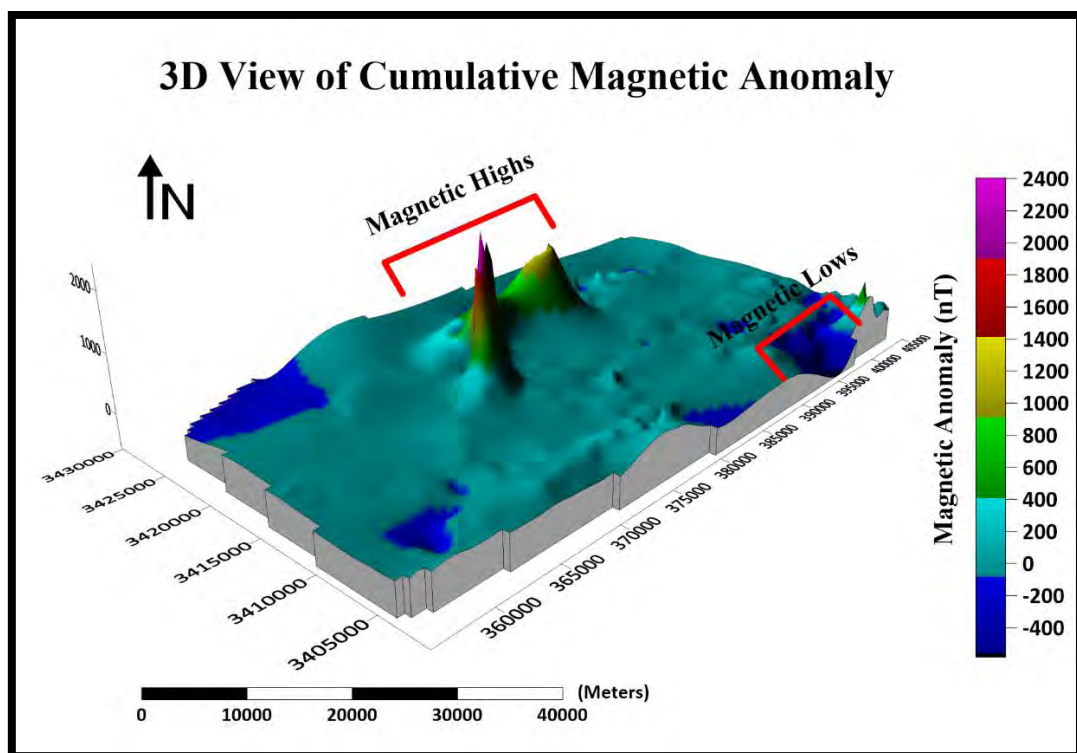


**Figure 4.7:** 3D Visualization of cumulative magnetic anomaly which clearly separates magnetic highs and lows as marked in the figure.

This visualization further validates the magnetic anomaly map, which showcases the combined impact, as depicted in Figure 4.5. The presence of magnetic highs is evident in

the study area, indicating the occurrence of high magnetic bodies within the anomalous zone. The 3D map of the anomalous zone exhibits distinct manifestations of magnetic lows. Magnetic highs are visually depicted by a color spectrum ranging from green to pink, indicating anomalies within the range of 600 nT to 2400 nT. The observed elevated anomalies are believed to be associated with ultramafic igneous rocks that include chromite rich in iron. Magnetic lows are visually represented by a blue tint, denoting magnetic anomalies that span a range of -200 nT to -600 nT. The studied area exhibits magnetic low zones that are indicative of nonmagnetic characteristics, which are commonly associated with the presence of sulphide mineralization. The intermediate magnetic anomaly values seen between the extremes of high and low magnetic readings are indicative of the presence of sedimentary rock formations, including sandstone, limestone, conglomerate, siltstone, and shale, within the research area.

#### 4.10 TMI Map of Digitized High Anomalous Zone

In order to effectively visualize the geometric and continuous magnetic behavior inside the research region, the high magnetic or anomalous zone has been digitized, as depicted in Figure 4.8. The primary objective of digitalization is to concentrate on areas with high mag-

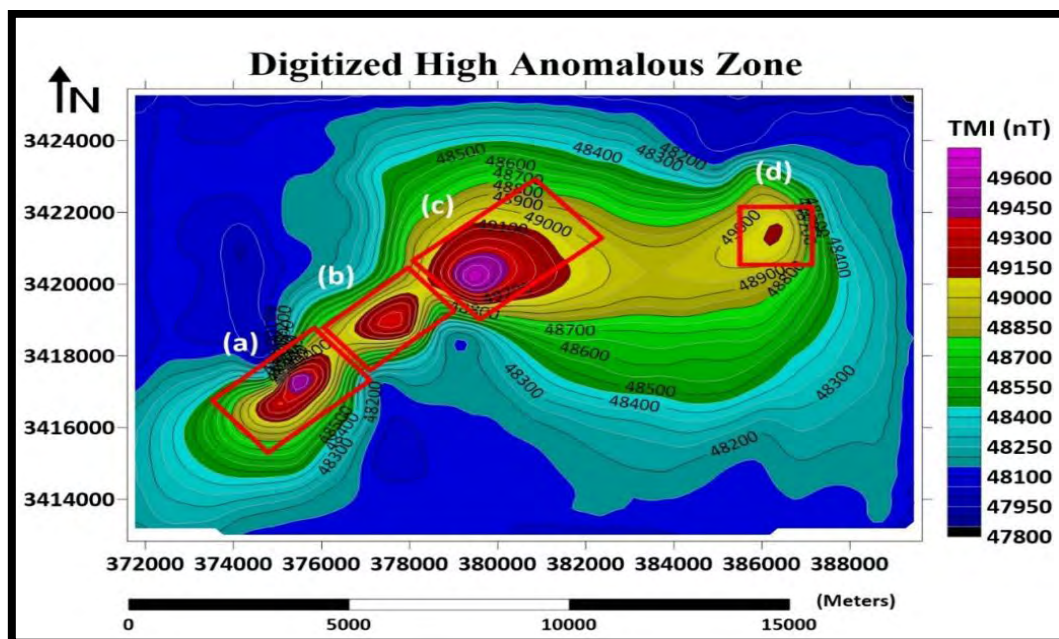


Figure 4.8: Digitized TMI map specifying high magnetic/ anomalous zone indicated by rectangles (a), (b), (c) and in the study area.

netic bearing or potential magnetic bodies inside the anomalous region of the designated study area. In this arrangement, a series of objects with high magnetization are positioned in a linear formation. Rectangles (a), (b), and (c) represent three distinct bodies characterized by significant magnetization and possessing elevated magnetic properties. The rectangle denoted as (d) exhibits little data regarding its magnetic properties, characterized by high values. Additionally, it is situated within a region that displays a significant concentration of anomalies. The magnetic data currently accessible exhibits low resolution due to the significant separation between survey stations. The prominence of these high anomalous zones can be enhanced through the implementation of a comprehensive magnetic survey throughout this geographical area.

#### 4.11 Superposition of Digitized Anomalous Zone and Geological Map of Study Area

The contour map of a high magnetic zone is overlaid onto the geology map of the study area (Figure 4.9). The high anomalous zone exhibits a significant degree of overlap with the thrust zone within the area under investigation. The region under consideration has a notable prevalence of intense tectonic processes. This zone is composed of a multitude of

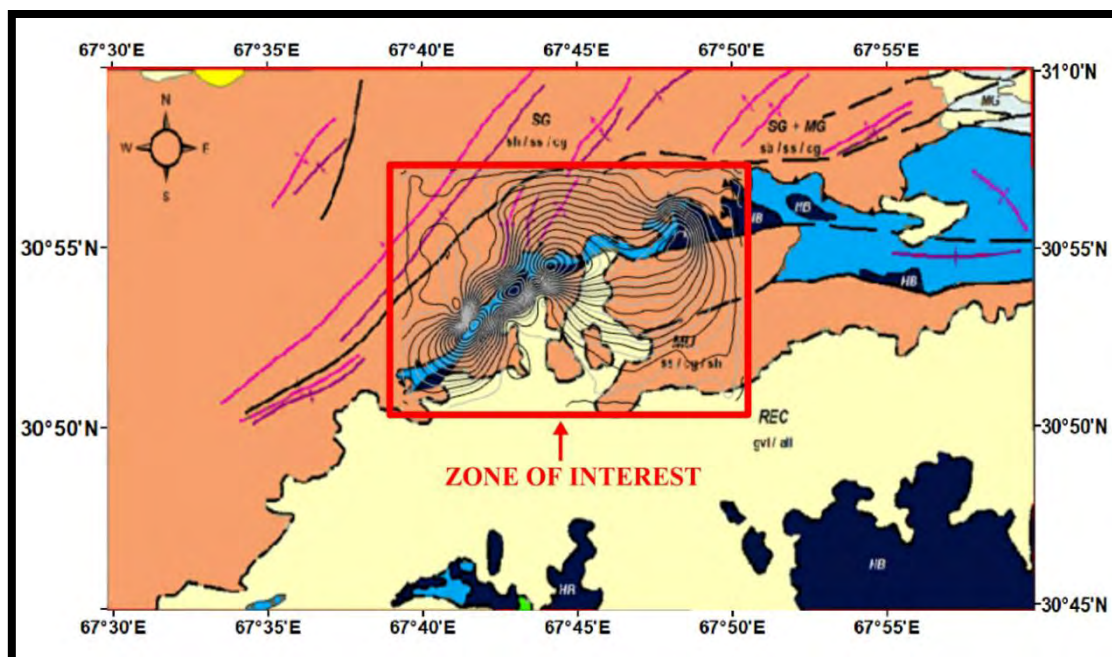


Figure 4.9: Overlay of high magnetic zone contour map on geological map of study area highlighting zone of interest.

separate ophiolite bodies and sedimentary rocks. The correlation between the presence of metallic ore bodies and ophiolites in this particular region of the research area is directly associated with a significant magnetism. Consequently, the alignment of high value contours exhibits a strong correlation with the region characterized by thrust faulting, which encompasses both ultramafic and sedimentary rock formations. The confirmation of a zone of interest in the research region is substantiated by the overlaying of two maps.

**CHAPTER 05**  
**MAGNETIC ATTRIBUTES**



## 5.1 Introduction

The magnetic response of anomalous ore bodies varies in both shape and magnitude location, strength and direction of magnetization, ore body's geometry, and the measured field's component (Aina, 1986). Magnetic data interpretation is therefore substantially complex compared to gravity data since the magnitude and shape of the anomaly varies and the anomalous response is not positioned directly above the ore body. However, the total magnetic field anomaly of a symmetric anomalous body, when observed at the polar region (exceedingly high latitude) or at the equator (extremely low latitude) is symmetrically located just vertically above the body (Aina, 1986). The trend at any other latitude is asymmetric and horizontally shifted. A magnetic transformation was devised by Baranov 1957, which converted the asymmetric total field anomalies into symmetric ones as if the anomaly were reduced to a pole. Subsequently, studies on transformation methods were applied by many, namely, LeMouel et al. 1974, Baranov 1975, and Hildenbrand 1983. Based on the general equation for magnetic transformation, Roy and Aina, 1986 established another transform named as reduction to equator, where the total magnetic field anomaly for a symmetric ore body is symmetric and has zero horizontal shift (although with a negative sign).

In magnetic method is a measure of the magnetic anomalies in the subsurface based on the contrast in their susceptibility (Harimei, 2019). Any field of interest contains potential anomalies in the form of highly susceptible bodies surrounded by faint susceptibility values depicting the country rocks. The magnetic trends of the anomalous bodies can be segregated from the surrounding rocks in the form of residual and regional anomalies (Broto and Putranto, 2011). The separation of the residual from the regional trends provides a better understanding of the subsurface, resulting in an accurate interpretation (Nugraha et al., 2016). These trends can be separated using different methods, one of which is the upward continuation method. A general continuation can be achieved using surface integrals, allowing detailed mapping of complex fields (Henderson and Zietz, 1949). The success of the method depends on the number of points used in computation as well as the arial extent and complexity of the subsurface anomalous bodies (Henderson and Zietz, 1949). The method, being cost effective and robust, is an excellent alternative to multi-level aeromagnetic acquisition (Henderson and Zietz, 1949). Researchers have

successfully used this method in studies, namely, Satiawan 2008, Purnomo et al. 2013, Hiskiawan 2016, and Nurdin et al. 2017.

Separation of the residual from the regional trend does increase the interpretability of the data. The anomalies and shallow structures, however, can be further enhanced and delineated using vertical and horizontal derivatives (Pal et al., 2016). Among others, Gonenc 2014, Pal and Majumdar 2015, and Vaish and Pal, 2015 have applied these methods in their respective studies. Application of the derivative techniques increases the component of an anomaly field pertaining to the higher wave number and subsequently reduces the complexities in anomaly data, thereby enhancing the visualization of the affiliated structures (Ravat 1996; Khalil 2012). The mathematical derivation of the vertical derivatives was conducted using reduced to pole data with the first vertical derivative being derived from the computation of the second horizontal derivatives of the first vertical derivative and by using Laplace equation (Fedi and Florio 2002).

## **5.2 Residual Magnetic Anomaly Map**

The initial stage in the production of a Residual Magnetic Anomaly Map involves commencing with a Total Magnetic Intensity Map. The Total Magnetic Intensity Map presents the raw magnetic field data collected from multiple locations within a surveyed region.

The estimation of the regional or background magnetic field was conducted by the utilization of a second order polynomial regression technique. This estimated field was then subtracted from the overall corrected magnetic intensity data, which predominantly arises from the magnetic properties of the Earth and geological characteristics, such as crustal magnetization, as depicted in. The inclusion of this stage is necessary as the presence of regional variations in the magnetic field can potentially mask subtle magnetic anomalies that have significance, hence posing challenges in their detection.

Figure 5.1 displays a residual anomaly map that illustrates variations in magnetic anomalies, both higher and lower, along with the inclusion of survey location plots. The

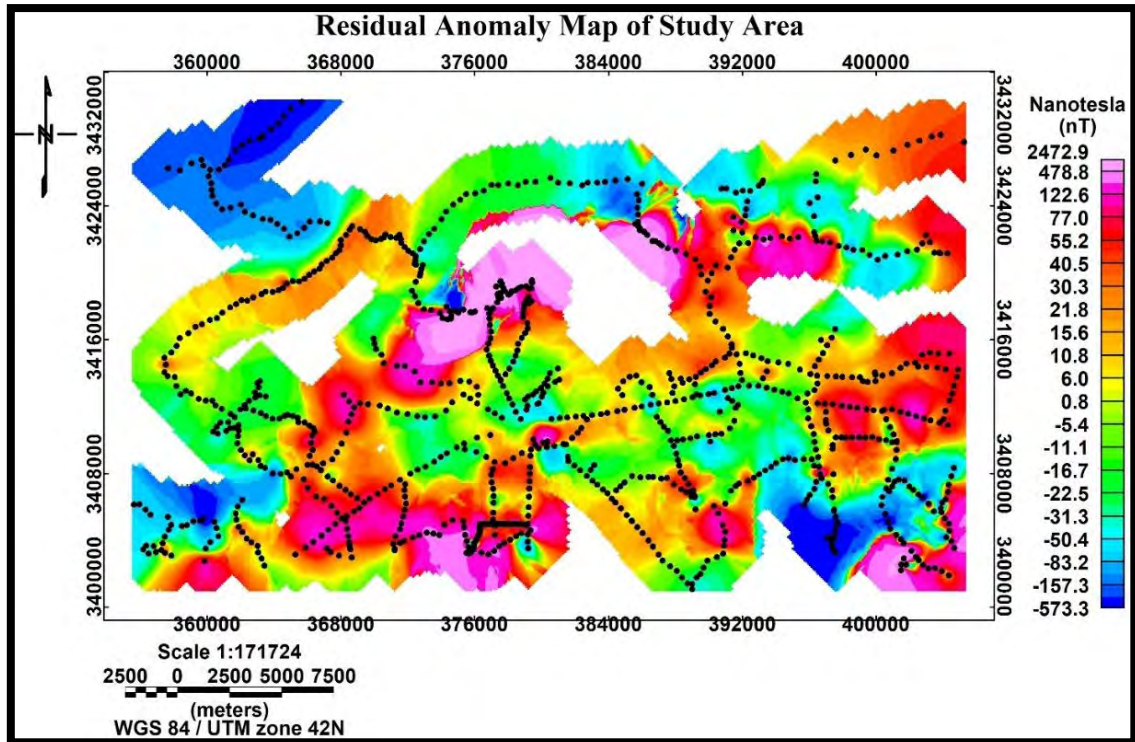


**Figure 5.1:** Residual magnetic anomaly map highlighting magnetic observation points. Pink color indicates higher residual magnetic anomalies while blue color lower anomalies.

presence of white spaces on the map can be attributed to the absence of data points inside the study area. The research area is characterized by a rough topography, particularly in mountainous regions, which poses significant challenges for surveyors due to limited accessibility.

### 5.3 Interpolated Residual Magnetic Anomaly Map

The regional magnetic field was computed using a second order polynomial regression approach. The Kriging interpolation method was utilized to do the interpolation of observed magnetic readings and computed magnetic values. Subsequently, the magnetic values that were determined through calculations were subtracted from the observed readings, so enabling the computation of the interpolated residual magnetic anomaly. In Figure 5.2, magnetic zones are depicted with pink tint. The map exhibits a notable presence of areas with high levels of anomalies. The region exhibiting elevated levels of magnetism is situated about at

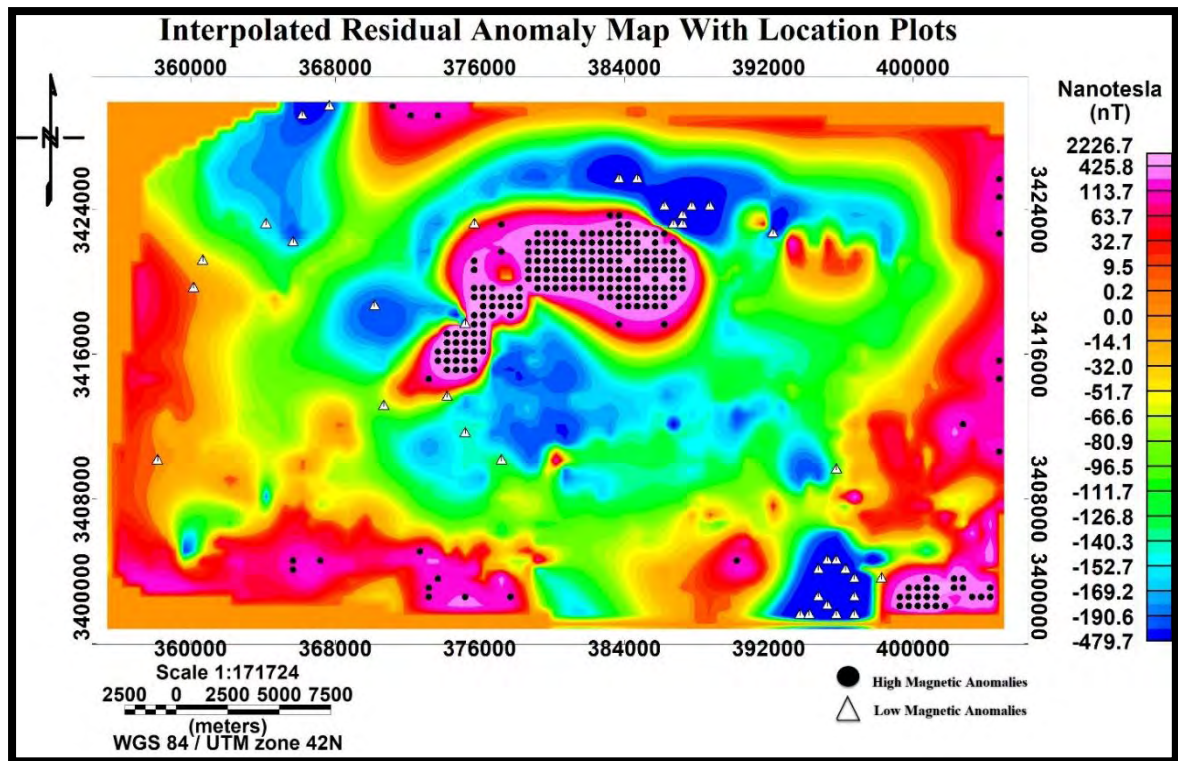


**Figure 5.2:** Interpolated Residual Anomaly map with location plots. Black dots represent high magnetic readings and white triangles low magnetic values.

the geographical midpoint of the map. The designated area is characterized by a concentration of black dots that represent significant magnetic anomalies. The research area exhibits notable low magnetic zones, which are visually represented by blue coloration accompanied by the presence of white triangles overlaying the blue regions. These white triangles serve to indicate areas with low magnetic values.

#### 5.4 Reduced to Magnetic Equator (RTE) Anomaly Map

The "Reduce to Equator Magnetic Anomaly Map" is a geophysical map that displays magnetic anomalies in a manner that replicates their visual representation if observed directly above the magnetic field source on the Earth's surface. The modifications made to this map in order to accommodate the inclination and declination of the magnetic field have greatly enhanced the ability to detect magnetic anomalies associated with subsurface features. According to Salapare et al. (2015), when dealing with magnetic data obtained at low magnetic latitudes or at the equator, it is more advantageous to utilize the

solution of the Reduction to Equator (RTE) rather than opting for the reduction to the pole method.

The process of data reduction is beneficial for the analysis of magnetic anomalies as it helps to eliminate mistakes arising from increased north-south amplitude signals, which are commonly observed during reduced-to-the-pole (RTP) operations. This conversion demonstrates significant benefits in the field of magnetic exploration, as well as in the domain of geological research.

The process of reducing to the equator was conducted by employing the specified parameters to delineate the magnetic field of the Earth inside the designated research region. The inclination of the geomagnetic field was used to be 49.2 degrees, while the declination was found to be 2.4 degrees.

The map illustrated in Figure 5.3 represents the result of the reduction to equator analysis. After implementing the Reduction to Equator (RTE) technique, the regions that have anom-

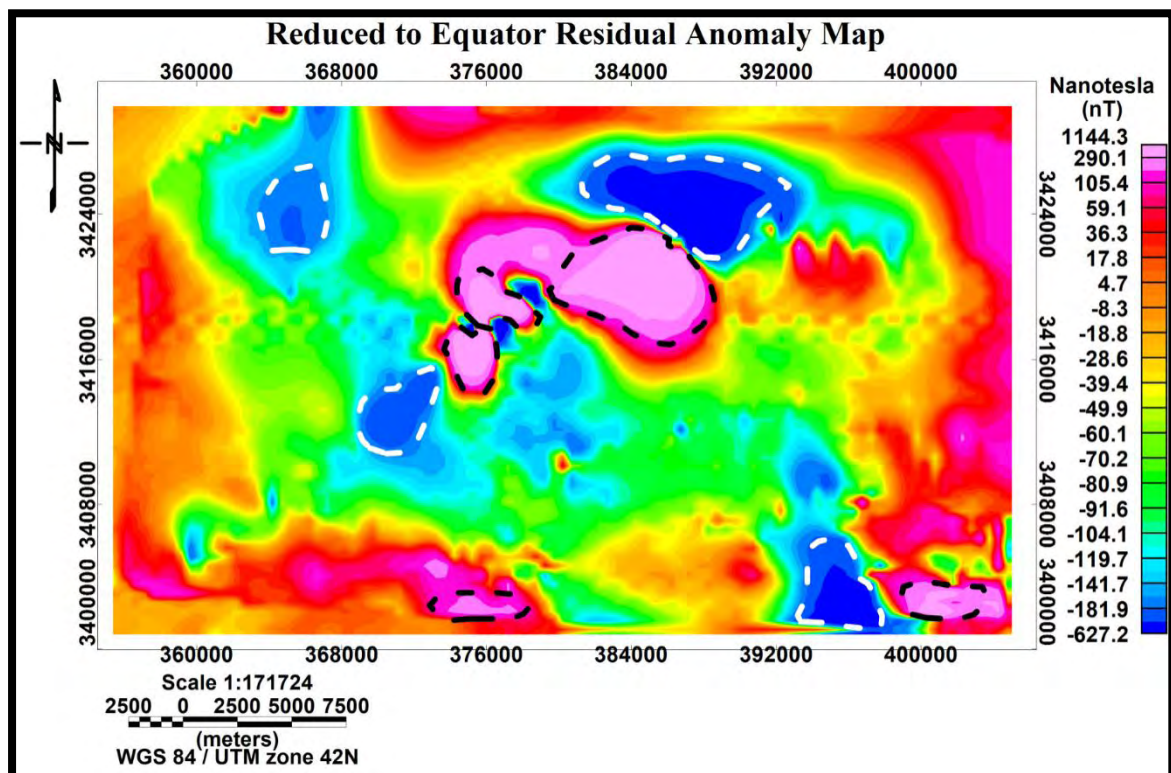


**Figure 5.3:** Shows residual magnetic anomaly reduced to equator. The map clearly delineates high and low magnetized zones marked with black and white dotted polygons respectively.

lies demonstrate a heightened level of significance within the specified study area. The aforementioned feature serves as a reliable means of differentiating the areas with high anomalies from those with low anomalies, as depicted on the map within the specified study region. Polygons were used to demarcate the areas of high and low anomalies on the map. The map displays black dotted polygons to represent magnetic bodies and white dotted polygons to indicate areas of low magnetization within the study area.

## 5.5 Upward Continuation Map

The upward continuation technique is employed to extend the acquired data from a specific elevation to a higher elevation. The aforementioned procedure leads to the attenuation of high-frequency characteristics when the data is displaced from the initial anomaly (Mekonnen, 2004). In essence, the technique of upward continuation is utilized to accentuate and underscore prominent geological characteristics, particularly those situated at deeper levels within the examined region.

The application of the upward continuation technique was utilized in order to minimize the impact of shallow sources on the reduced to equator magnetic anomalies. The selected height value for the execution of upward continuation was 300 meters above the Earth's surface (Figure 5.4).

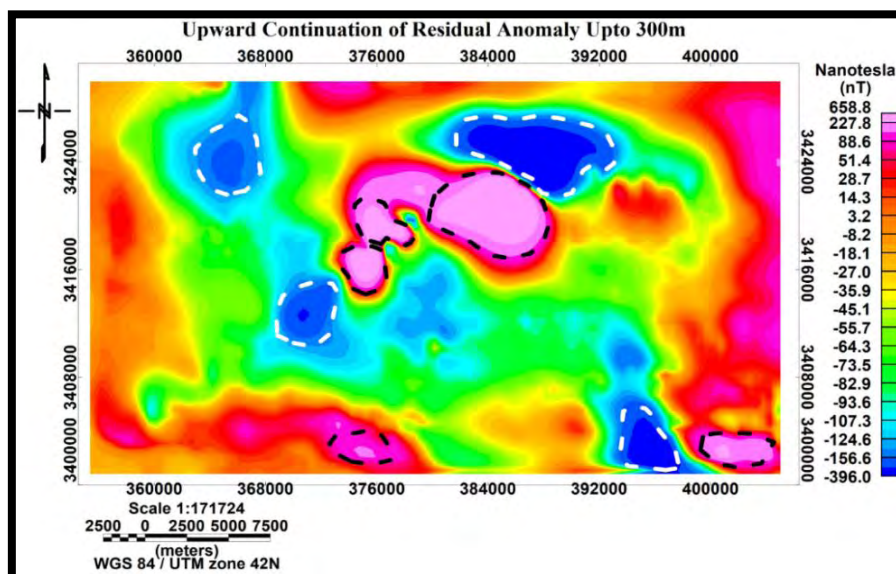


**Figure 5.4:** Reduced to Equator anomaly upward continued to 300 m elevation. It separated anomalous zones into distinct high magnetized zones.

The method of upward continuation was applied at several elevation thresholds, specifically at 200, 300, 400, and 500 meters. The utilization of the map effectively improved the discernibility of both the elevated and diminished irregularities inside the designated area, while simultaneously eradicating any superficial disruptions present on the surface. The process of upward continuation mapping involves the division of particularly elevated magnetic zones into many zones, which appear to consist of magnetized bodies located in close proximity to one another. The map illustrates the existence of magnetic bodies, with areas of strong and low magnetism represented by black and white dotted polygons, respectively.

## 5.6 First Order Vertical Derivative Map

The first vertical derivative is a filtering technique commonly employed in the analysis of magnetic data. Its purpose is to amplify the vertical extent of anomalies while simultaneously reducing their lateral extent. This observation emphasizes the subtle variations in the vertical gradient of magnetic field strength as a function of depth under the Earth's surface. The primary use of the first vertical derivative is the identification of borders of geological formations and magnetic and non-magnetic entities in the subsurface. The utilization of this instrument also introduces extraneous data. Upon the implementation of this technique on the residual anomaly of the RTE, Figure 5.6 depicts the effective parti-

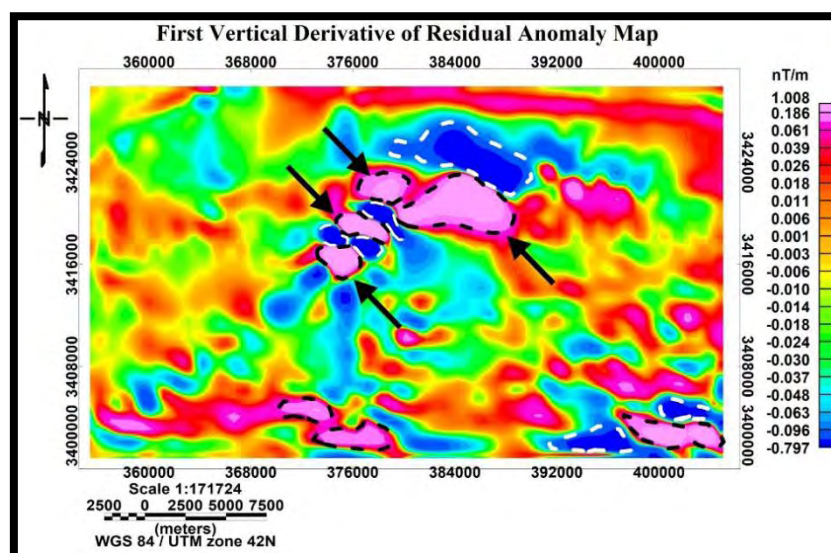


**Figure 5.5:** First order vertical derivative map representing distinct high and low anomalous zones with black and white polygons respectively. The distinct high anomalous zones are highlighted with arrows.

tioning of the anomalous zone into subzones. The findings provide evidence for the presence of distinct magnetic entities within the investigated region. The black dotted polygons represent areas characterized by high magnetization, whereas the white dotted polygons represent areas characterized by low magnetization.

## 5.7 Horizontal Derivative Map

This filter is a crucial tool utilized to process prospective field data, including gravity and magnetic data. The primary objective of this filter is to determine the spatial boundaries or interfaces of geological formations inside the subsurface. In this investigation, the aforementioned attribute is utilized with the same objective in consideration. The utilization of the horizontal derivative introduces a certain level of high wavelength noise into the resulting map. In order to address this concern, a low pass or high-cut filter was implemented to decrease the residual anomaly map at the equator (Figure 5.6). The resulting map illustrates the fragmentation of the primary anomalous region into distinct zones. The primary areas of focus are indicated by arrows on the map.

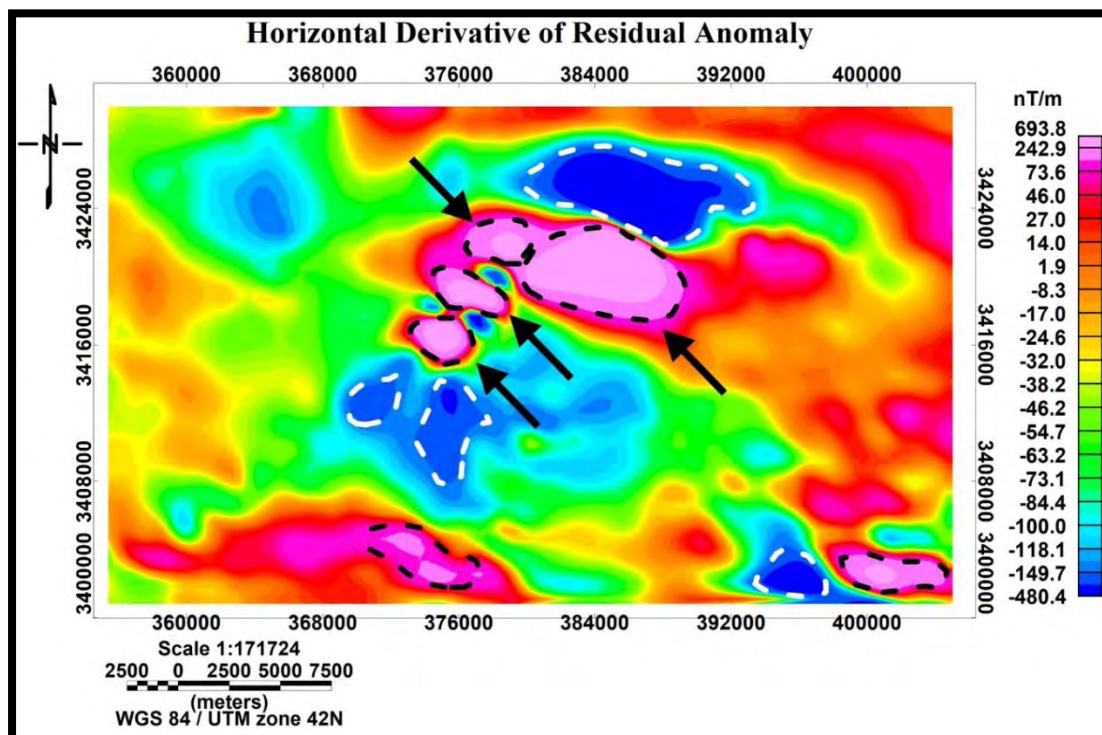


**Figure 5.6:** Horizontal derivative map representing variation of magnetic intensity values spatially within the study area. Black dotted polygons indicate a high magnetized zone and white polygons the lower magnetized zone.



The feasibility of this approach was facilitated through the use of a horizontal derivative technique on the dataset pertaining to the designated study region. Black color dotted polygons are used to indicate areas with high magnetization, whereas dotted white polygons are employed to represent regions with lesser magnetization.

**CHAPTER 06**

**DISCUSSIONS, CONCLUSIONS AND  
RECOMMENDATIONS**

## 6.1 Discussions

The utilization of geophysical data, when combined with geological knowledge, has made a substantial contribution towards comprehending the tectonic history and evolution of numerous well-known ophiolites throughout the globe (e.g., Manghnani & Coleman, 1981; Ricci et al., 1985; Godfrey et al., 1997; Zaigham & Mallick, 2000). The utilization of magnetic data has been employed to impose constraints on several aspects of emplaced lithospheric fragments, including their thickness, growth, subsurface geometry, and the prospect of mineralization. In comparison to places that offer comprehensive and precise magnetic data, such as the spreading centers observed in mid-ocean ridges, the study area suffers from a shortage of data that limits the precise identification of discrete blocks displaying normal or reverse polarities (Leroy et al., 2000). The magnetic anomalies observed in the Ultramafic rocks of the Muslim Bagh Ophiolite Belt are attributed only to the horizontal and vertical anomalies present among the different lithological units.

The analysis of magnetic data is conducted using a two-step process. The initial phase involves the regional analysis, followed by the subsequent division of the data into maps depicting regional and residual magnetic anomalies within the designated study area. The residual magnetic anomaly map undergoes additional processing to provide maps that enhance the existing anomalous body. These maps include upward continuation, vertical derivative, and horizontal derivatives.

A semi-detailed magnetic survey was undertaken in Muslim Bagh in order to investigate the presence of metallic minerals. The survey involved the establishment of observation stations at intervals of 300 to 600 meters. Upon analysis of the semi-detailed magnetic data, significant anomalies were observed in the thrust zone and the north Muslim Bagh ophiolites, exhibiting a strong correlation with the geological map of the study area. The process of magnetic mapping has effectively delineated a region of elevated magnetic intensity that extends from toposheets 34N/9 to 34N/13. The Surfer-20 software was utilized for the generation of cumulative magnetic and total magnetic intensity (TMI) maps. The magnetic anomaly map displayed a range of high anomalies ranging from 520 to 2480 nT, as well as low anomalies ranging from -40 to -600 nT as shown in Figure 4.5. The cumulative total magnetic intensity (TMI) map was generated using a similar methodology,

revealing elevated total magnetic intensities ranging from 48620 to 50540 nT, as well as lower total magnetic intensities ranging from 47500 to 48140 nT as shown in Figure 4.6. Significant magnetic anomalies and high total magnetic intensity values are observed in the presence of iron ores and other metallic minerals (Salapare et al., 2015). The presence of low magnetic zones in the southern portion of the research region, characterized by low magnetic anomalies and low overall magnetic intensity values, is often associated with sulphide mineralization or minerals located in valleys.

Additionally, the limits of comparing magnetic signatures are only determined by the units available inside the designated study region. The magnetic anomaly map generated by the RTE method exhibits distinct divisions into two magnetic terranes. The first terrain, characterized by high anomalies, is represented by a pink color and extends the southwest to northeast region of the study area. Conversely, the second terrain displays low magnetic anomalies and is observed in vicinity of the high anomalous body, depicted by a blue color in Figure 5.3.

After doing the above processes, still some shallow source noise is present. To overcome these problems Upward continuation, Horizontal and vertical derivative is applied to RTE (Reduced to Equator) residual anomaly map. The primary applications of upward continuation involve the adjustment of observation altitudes to a reference point, known as a datum, in order to facilitate the interpretation of a survey. This is particularly relevant in the context of the crustal magnetic field. Additionally, this concept is utilized to decrease data with short wavelengths. The noise is amplified when the field is extended vertically, and the horizontal dimension is expanded (Courtillet et al., 1978; Shure et al., 1982; Fedi et al., 1999, Blakely, 1995). The Upward Continuation map depicted in Figure 5.4 demonstrates the suppression of shallow level noises inside the study area, while simultaneously enhancing the anomaly located in the middle section. The First vertical derivative map and Horizontal Derivative Map depicted in Figure 5.5 and 5.6 delineate the boundaries of an anomalous zone in the vertical direction and Horizontal direction respectively.

## 6.2 Conclusions

- The study region is constrained by a lack of adequate magnetic data, which restricts the precise identification of distinct blocks displaying normal or reverse polarity.
- The subsequent examination of the semi-detailed magnetic data revealed considerable anomalies, namely in the thrust zone and the northern Muslim Bagh ophiolites, which closely corresponded with the geological map. The utilization of magnetic mapping successfully demarcated a region characterized by an elevated level of magnetic intensity.
- The examination of Total Magnetic Intensity maps highlighted a range of magnetic anomalies and corresponding total magnetic intensity values, particularly linked to ultramafic rocks within the designated research region. The southern portion of the research area exhibits lower magnetic zones characterized by diminished magnetic anomalies and overall magnetic intensity values. These zones have frequently been associated with the presence of sulphide mineralization or minerals situated within valleys.
- A magnetic anomaly map made using the RTE approach showed two separate terranes: one with raised anomalies diagonally from southwest to northeast in pink, and the other with lower anomalies centered around a high anomalous body in blue.
- The utilization of noise reduction methodologies, such as upward continuation and derivatives, has proven to be a successful approach in mitigating shallow source noise, resulting in improved visibility and accuracy in the interpretation of geophysical data.

## 6.3 Recommendations

- In toposheets 34N/9 and 34N/13, a high magnetic zone delineated by a semi-detailed magnetic survey is indicated for a detailed magnetic survey to explore metallic mineralization and geometrical calculations of an anomalous body.
- Low magnetic zone is recommended for Induced Polarization (IP) technique to investigate the nonmagnetic minerals.
- For chromite exploration, an electromagnetic survey is advised for correlation and validation with magnetic results.

## REFERENCES

- Abedi, M., Gholami, A., & Norouzi, G. H. (2013). A stable downward continuation of airborne magnetic data: A case study for mineral prospectivity mapping in Central Iran. *Computers & Geosciences*, 52, 269-280.
- Aboud, E., Salem, A., & Mekkawi, M. (2011). Curie depth map for Sinai Peninsula, Egypt deduced from the analysis of magnetic data. *Tectonophysics*, 506(1-4), 46-54.
- Abubakar, R., Muxworthy, A. R., Sephton, M. A., Southern, P., Watson, J. S., Fraser, A. J., & Almeida, T. P. (2015). Formation of magnetic minerals at hydrocarbon-generation conditions. *Marine and Petroleum Geology*, 68, 509-519.
- Adagunodo, T. A., Sunmonu, L. A., & Adeniji, A. A. (2015). An overview of magnetic method in mineral exploration.
- Ahmed, Z. (1996). Nd-and Sr-isotopic constraints and geochemistry of the Bela Ophiolite-Melange complex, Pakistan. *International Geology Review*, 38(4), 304-319.
- Aina, A. (1986). Reduction to equator, reduction to pole and orthogonal reduction of magnetic profiles. *Exploration Geophysics*, 17(3), 141-145.
- Al-Farhan, M., Oskooi, B., Ardestani, V. E., Abedi, M., & Al-Khalidy, A. (2019). Magnetic and gravity signatures of the Kifl oil field in Iraq. *Journal of Petroleum Science and Engineering*, 183, 106397.
- Al-Garni, M. (2011). Magnetic and DC resistivity investigation for groundwater in a complex subsurface terrain. *Arabian Journal of Geosciences*, 4.
- Allemann, F. R. A. N. Z. (1979). Time of emplacement of the Zhob Valley ophiolites and Bela ophiolites, Baluchistan (preliminary report). *Geodynamics of Pakistan. Geological Survey of Pakistan, Quetta*, 215-242.
- Araffa, S. A. S., Helaly, A. S., Khozium, A., Lala, A. M., Soliman, S. A., & Hassan, N. M. (2015). Delineating groundwater and subsurface structures by using 2D resistivity, gravity

and 3D magnetic data interpretation around Cairo–Belbies Desert road, Egypt. *NRIAG Journal of Astronomy and Geophysics*, 4(1), 134-146.

Baranov, V. (1957). A new method for interpretation of aeromagnetic maps: pseudo-gravimetric anomalies. *Geophysics*, 22(2), 359-382.

Baranov, W. (1975). Potential fields and their transformations in applied geophysics.

Bender, F., & Raza, H. A. (1995). Geology of Pakistan.

Bilgrami, S. A. (1964). *Mineralogy and petrology of the central part of the Hindubagh igneous complex, Hindubagh mining district, Zhob Valley, West Pakistan*. Government of Pakistan Press.

Blakely, R. J. (1995). Potential Theory in Gravity and Magnetic Applications. Cambridge University, Cambridge.

Broto, S., & Putranto, T. T. (2011). Aplikasi Metode Geomagnet Dalam Eksploasi Panasbumi. *TEKNIK*, 32(1), pp. 79-87.

Cooper, G. R. J., & Cowan, D. R. (2004). Filtering using variable order vertical derivatives. *Computers & Geosciences*, 30(5), 455-459.

Courtillot, V., Ducruix, J., & Le Mouel, J. L. (2005). Inverse methods applied to continuation problems in geophysics. In *Applied Inverse Problems: Lectures presented at the RCP 264 "Etude Interdisciplinaire des Problèmes Inverses"*, sponsored by the Centre National de la Recherche Scientifique (pp. 48-82). Berlin, Heidelberg: Springer Berlin Heidelberg.

Dentith, M., & Mudge, S. T. (2014). *Geophysics for the mineral exploration geoscientist*. Cambridge University Press.

Di Maio, R., La Manna, M., Piegari, E., Zara, A., & Bonetto, J. (2018). Reconstruction of a Mediterranean coast archaeological site by integration of geophysical and archaeological data: The eastern district of the ancient city of Nora (Sardinia, Italy). *Journal of Archaeological Science: Reports*, 20, 230-238.

Dunstan, S., Rosenbaum, G., & Babaahmadi, A. (2016). Structure and kinematics of the Louth-Eumarra Shear Zone (north-central New South Wales, Australia) and implications for the Paleozoic plate tectonic evolution of eastern Australia. *Australian Journal of Earth Sciences*, 63(1), 63-80.

Elhussein, M., & Shokry, M. (2020). Use of the airborne magnetic data for edge basalt detection in Qaret Had El Bahr area, Northeastern Bahariya Oasis, Egypt. *Bulletin of Engineering Geology and the Environment*, 79, 4483-4499.

Essa, K. S., & Elhussein, M. (2017). A new approach for the interpretation of magnetic data by a 2-D dipping dike. *Journal of Applied Geophysics*, 136, 431-443.

Essa, K. S., & Elhussein, M. (2019). Magnetic interpretation utilizing a new inverse algorithm for assessing the parameters of buried inclined dike-like geological structure. *Acta Geophysica*, 67, 533-544.

Farah, A., & DeJong, K. A. (1979). Geodynamics of Pakistan. Geological Survey of Pakistan.

Fedi, M., & Florio, G. (2002). A stable downward continuation by using the ISVD method. *Geophysical Journal International*, 151(1), 146-156.

Fedi, M., Rapolla, A., & Russo, G. (1999). Upward continuation of scattered potential field data. *Geophysics*, 64(2), 443-451.

Ganiyu, S. A., Badmus, B. S., Awoyemi, M. O., Akinyemi, O. D., & Olurin, O. T. (2013). Upward continuation and reduction to pole process on aeromagnetic data of Ibadan Area, South-Western Nigeria. *Earth Science Research*, 2(1), 66.

Gansser, A. (1974). Himalaya. *Geological Society, London, Special Publications*, 4(1), 267-278.

Gnos, E., Immenhauser, A., & Peters, T. J. (1997). Late Cretaceous/early Tertiary convergence between the Indian and Arabian plates recorded in ophiolites and related sediments. *Tectonophysics*, 271(1-2), 1-19.



Godfrey, N. J., Beaudoin, B. C., & Klemperer, S. L. (1997). Ophiolitic basement to the Great Valley forearc basin, California, from seismic and gravity data: Implications for crustal growth at the North American continental margin. *Geological Society of America Bulletin*, 109(12), 1536-1562.

Gönenç, T. (2014). Investigation of distribution of embedded shallow structures using the first order vertical derivative of gravity data. *Journal of Applied Geophysics*, 104, 44-57.

Harimeï, B. (2019, August). Analysis of Regional Anomaly on Magnetic Data Using the Upward Continuation Method. In *IOP Conference Series: Earth and Environmental Science* (Vol. 279, No. 1, p. 012037). IOP Publishing.

Henderson, R. G. (1960). A comprehensive system of automatic computation in magnetic and gravity interpretation. *Geophysics*, 25(3), 569-585.

Henderson, R. G., & Zietz, I. (1949). The upward continuation of anomalies in total magnetic intensity fields. *Geophysics*, 14(4), 517-534.

Hinze, W. J., Von Frese, R. R., Von Frese, R., & Saad, A. H. (2013). *Gravity and magnetic exploration: Principles, practices, and applications*. Cambridge University Press.

Hiskiawan, P. (2016). Pengaruh Pola Kontur Hasil Kontinuasi Atas pada Data Geomagnetik Intepretasi Reduksi Kutub. *saintifika*, 18(1), 9-9.

Iqbal, M. (2004). Integration of Satellite Data and Field Observations in Pishin Basin, Balochistan. *Pakistan Journal of Hydrocarbon Research*, 14, 1-17.

Jadoon, I. A., & Khurshid, A. (1996). Gravity and tectonic model across the Sulaiman fold belt and the Chaman fault zone in western Pakistan and eastern Afghanistan. *Tectonophysics*, 254(1-2), 89-109.

Jeng, Y., Lee, Y. L., Chen, C. Y., & Lin, M. J. (2003). Integrated signal enhancements in magnetic investigation in archaeology. *Journal of Applied Geophysics*, 53(1), 31-48.

Jones, A. G. (1961). Reconnaissance geology of part of West Pakistan: a Columbo Plan cooperative project. *Hunting Survey Corporation, Government of Canada, Toronto*.

Jones, A. G., Manistre, B. E., Oliver, R. L., Willson, G. S., & Scott, H. S. (1960). Reconnaissance Geology of part of West Pakistan (Colombo Plan co-operative project conducted and compiled by Hunting Survey Corporation). *Government of Canada, Toronto, 550.*

Joshua, E. O., Layade, G. O., Akinboboye, V. B., & Adeyemi, S. A. (2017). Magnetic mineral exploration using ground magnetic survey data of Tajimi Area, Lokoja. *Global Journal of Pure and Applied Sciences, 23(2), 301-310.*

Kakar, M. I. (2011). Petrology, geochemistry and tectonic setting of the Muslim Bagh ophiolite, Balochistan, Pakistan. *Unpublished Ph. D. Thesis, Centre of Excellence in Mineralogy, University of Balochistan, Quetta, 265.*

Kasi, A. K., Kassi, A. M., Umar, M., Manan, R. A., & Kakar, M. I. (2012). Revised lithostratigraphy of the Pishin Belt, northwestern Pakistan. *Journal of Himalayan Earth Science, 45(1).*

Kazmi, A. H., & Abbas, S. G. (2001). Metallogeny and mineral deposits of Pakistan. *Islamabad: Orient Petroleum Inc, 88-150.*

Kazmi, A. H., & Jan, M. Q. (1997). Geology and tectonics of Pakistan. *(No Title).*

Kearey, P., Brooks, M., & Hill, I. (2002). *An introduction to geophysical exploration* (Vol. 4). John Wiley & Sons.

Khalil, M. H. (2012). Magnetic, geo-electric, and groundwater and soil quality analysis over a landfill from a lead smelter, Cairo, Egypt. *Journal of Applied Geophysics, 86, 146-159.*

Khan, S. D., Mahmood, K., & Casey, J. F. (2007). Mapping of Muslim Bagh ophiolite complex (Pakistan) using new remote sensing, and field data. *Journal of Asian Earth Sciences, 30(2), 333-343.*

Konadu Amoah, B., Dadzie, I., & Takyi-Kyeremeh, K. (2018). Integrating gravity and magnetic field data to delineate structurally controlled gold mineralization in the Sefwi Belt of Ghana. *Journal of Geophysics and Engineering, 15(4), 1197-1203.*

Lawrence, R. D., & Yeats, R. S. (1979). Geological reconnaissance of the Chaman Fault in Pakistan. *Geodynamics of Pakistan*, 351-357.

Lawrence, R. D., Yeats, R. S., Khan, S. H., Farah, A., & DeJong, K. A. (1981). Thrust and strike slip fault interaction along the Chaman transform zone, Pakistan. *Geological Society, London, Special Publications*, 9(1), 363-370.

LeMouel, J. L., Courtillot, V. E., & Galdeano, A. (1974). A simple formalism for the study of transformed aeromagnetic profiles and source location problems. *Journal of Geophysical Research*, 79(2), 324-331.

Lenz, J. E. (1990). A review of magnetic sensors. *Proceedings of the IEEE*, 78(6), 973-989.

Leroy, S., Mauffret, A., Patriat, P., & Mercier de Lépinay, B. (2000). An alternative interpretation of the Cayman trough evolution from a reidentification of magnetic anomalies. *Geophysical Journal International*, 141(3), 539-557.

Lowrie, W., & Fichtner, A. (2020). *Fundamentals of geophysics*. Cambridge university press.

Mahmood, K., Boudier, F., Gnos, E., Monié, P., & Nicolas, A. (1995). <sup>40</sup>Ar/<sup>39</sup>Ar dating of the emplacement of the Muslim Bagh ophiolite, Pakistan. *Tectonophysics*, 250(1-3), 169-181.

Malkani, M. S., Mahmood, Z., Arif, S. J., & Alyani, M. I. (2017). Revised Stratigraphy and Mineral Resources of Balochistan Basin, Pakistan. *Geological Survey of Pakistan, Information Release, 1002*, 1-38.

Manghnani, M. H., & Coleman, R. G. (1981). Gravity profiles across the Samail ophiolite, Oman. *Journal of Geophysical Research: Solid Earth*, 86(B4), 2509-2525.

Maus, S., Sengpiel, K. P., Röttger, B., Siemon, B., & Tordiffe, E. A. W. (1999). Variogram analysis of helicopter magnetic data to identify paleochannels of the Omaruru River, Namibia. *Geophysics*, 64(3), 785-794.

Mekonnen, T. K. (2004, March). Interpretation and geodatabase of dykes using aeromagnetic data of Zimbabwe and Mozambique. ITC.

Middleton, M., Schnur, T., Sorjonen-Ward, P., & Hyvönen, E. (2015). Geological lineament interpretation using the object-based image analysis approach: results of semi-automated analyses versus visual interpretation. *Geological Survey of Finland, Special Paper, 57*, 135-154.

Nabighian, M. N., Grauch, V. J. S., Hansen, R. O., LaFehr, T. R., Li, Y., Peirce, J. W., ... & Ruder, M. E. (2005). The historical development of the magnetic method in exploration. *Geophysics, 70*(6), 33ND-61ND.

Nugraha, Y. A., Hiskiawan, P., & Supriyadi, S. (2016). Upward Continuation of Subsurface Anomalies Utilizing Magnetic Data in The Bedadung Watershed, Jember City. *Jurnal ILMU DASAR, 16*(2), 69-74.

Nurdin, N. H., Massinai, M. A., & Aswad, S. (2017). Identifikasi Pola Sebaran Intrusi Batuan Bawah Permukaan Menggunakan Metode Geomagnet Di Sungai Jenelata Kabupaten Gowa. *Jurnal Geoelebes, 1*(1), 17-22.

Nwankwo, L. I., Olasehinde, P. I., & Bayewu, O. O. (2007). Depth estimates from a ground magnetic survey across a North-South trending geologic structure in a part of the basement complex terrain of Ilorin, West of central Nigeria. *Global Journal of pure and applied sciences, 13*(2), 209-214.

Otsuki, K., Hoshino, K., Anwar, M., Mengal, J. M., Broahi, I. A., Fatmi, A. N., & Yuji, O. (1989). Breakup of Gondwanaland and emplacement of ophiolitic complexes in Muslim Bagh area of Balochistan, Pakistan. *Tectonics and sedimentation of the Indo-Eurasian colliding plate boundary region and its influence on the mineral development in Pakistan, Hiroshima University, 33-57*.

Pal, S. K., & Majumdar, T. J. (2015). Geological appraisal over the Singhbhum-Orissa Craton, India using GOCE, EIGEN6-C2 and in situ gravity data. *International Journal of Applied Earth Observation and Geoinformation, 35*, 96-119.

Pal, S.K., Vaish, J., Kumar, S., and Bharti, A.K., 2016. Coal fire mapping of East Basuria Colliery, Jharia coalfield using vertical derivative technique of magnetic data. *Journal of Earth System Science*, 125, pp.165-178.

Purnomo, J., Koesuma, S., & Yuniarto, M. (2013). Pemisahan anomali regional-residual pada metode gravitasi menggunakan metode moving average, polynomial dan inversion. *Indonesian Journal of Applied Physics*, 3(1), 10.

Qayyum, M., Lawrence, R. D., & Niem, A. R. (1997). Molasse-delta-flysch continuum of the Himalayan orogeny and closure of the Paleogene Katawaz remnant ocean, Pakistan. *International geology review*, 39(10), 861-875.

Qayyum, M., Niem, A. R., & Lawrence, R. D. (1996). Newly discovered Paleogene deltaic sequence in Katawaz basin, Pakistan, and its tectonic implications. *Geology*, 24(9), 835-838.

Ravat, D. (1996). Analysis of the Euler method and its applicability in environmental magnetic investigations. *Journal of Environmental and Engineering Geophysics*, 1(3), 229-238.

Ricci, M. P., Moores, E. M., Verosub, K. L., & McClain, J. S. (1985). Geologic and gravity evidence for thrust emplacement of the Smartville ophiolite. *Tectonics*, 4(6), 539-546.

Rossmann, D. L., Ahmad, Z., & Rehman, H. (1971). Geology and economic potential for chromite in the Zhob valley ultramafic complex (Jang Tor Ghar) Hindubagh, Quetta Division, West Pakistan. *Geol Surv and US Geol Surv Interim Report PK-51*.

Salapare, R. C., Dimalanta, C. B., Ramos, N. T., Manalo, P. C., Faustino-Eslava, D. V., Queaño, K. L., & Yumul Jr, G. P. (2015). Upper crustal structure beneath the Zambales Ophiolite Complex, Luzon, Philippines inferred from integrated gravity, magnetic and geological data. *Geophysical Journal International*, 201(3), 1522-1533.

Sarwar, G. (1992). Tectonic setting of the Bela Ophiolites, southern Pakistan. *Tectonophysics*, 207(3-4), 359-381.

Satiawan, S. (2009). Aplikasi Kontinuasi Ke Atas dan Filter Panjang Gelombang untuk Pemisahan Anomali Regional-Residual Pada Data Geomagnetik. *Tugas Akhir*.

Sengor, A. M. C. (1987). Tectonics of the Tethysides: orogenic collage development in a collisional setting. *Annual Review of Earth and Planetary Sciences*, 15(1), 213-244.

Sharma, P. V. (1985). Geophysical methods in geology.

Shure, L., Parker, R. L., & Backus, G. E. (1982). Harmonic splines for geomagnetic modelling. *Physics of the Earth and Planetary Interiors*, 28(3), 215-229.

Siddiqui, R. H., Aziz, A., Mengal, J. M., Hoshino, K., & Sawada, Y. (1996). Geology, Petrochemistry and tectonic evolution of Muslim Bagh ophiolite complex, Pakistan. In *Proc. Of Geoscience Colloquium, Geoscience Lab., GSP* (Vol. 16, pp. 11-46).

Sun, B., Dong, P., Wang, C., Pu, X., & Wu, Y. (2009). Quantitative analysis of magnetic anomaly of reinforcements in bored in-situ concrete piles  $\mathfrak{R}$ . *Applied Geophysics*, 6, 275-286.

Treloar, P. J., & Izatt, C. N. (1993). Tectonics of the Himalayan collision between the Indian plate and the Afghan block: A synthesis. *Geological Society, London, Special Publications*, 74(1), 69-87.

Vaish, J., & Pal, S. K. (2015). Geological mapping of Jharia Coalfield, India using GRACE EGM2008 gravity data: a vertical derivative approach. *Geocarto International*, 30(4), 388-401.

Vredenburg, E. W. (1901). A geological sketch of the Baluchistan desert, and part of eastern Persia. (*No Title*).

Weymouth, J. W. (1986). Geophysical methods of archaeological site surveying. In *Advances in archaeological method and theory* (pp. 311-395). Academic Press.

Wu, G., Zhang, C., & Yuan, Y. (2015, April). Interpretation of magnetic UXO data using a combined analytic signal and Euler method. In *International Workshop and Gravity, Electrical & Magnetic Methods and their Applications, Chenghu, China, 19-22 April*

2015 (pp. 240-243). Society of Exploration Geophysicists and Chinese Geophysical Society.

Zaher, M. A., Saibi, H., Mansour, K., Khalil, A., & Soliman, M. (2018). Geothermal exploration using airborne gravity and magnetic data at Siwa Oasis, Western Desert, Egypt. *Renewable and Sustainable Energy Reviews*, 82, 3824-3832.

Zaigham, N. A., & Mallick, K. A. (2000). Bela ophiolite zone of southern Pakistan: Tectonic setting and associated mineral deposits. *Geological Society of America Bulletin*, 112(3), 478-489.